SERDP

FINAL REPORT

Multi-Scale Evaluation of PFAS Thermal Destruction Requirements

Erin Shields, Jon Krug, William Linak, Stephen Jackson, William Roberson
United States Environmental Protection Agency
Office of Research and Development

Takahiro Yamada, Moshan Kahandawala
University of Dayton Research Institute

January 2025

SERDP Project ER21-1288

REPORT DOCUMENTATION PAGE

Form Approved
OMB No. 0704-0188

1. REPORT DATE *(DD-MM-YYYY)*	**2. REPORT TYPE**	**3. DATES COVERED** *(From - To)*
01-17-2024	Final Report	May 2021 – June 2024

4. TITLE AND SUBTITLE

Multi-Scale Evaluation of PFAS Thermal Destruction Requirements

5a. CONTRACT NUMBER

5b. GRANT NUMBER

5c. PROGRAM ELEMENT NUMBER

6. AUTHOR(S)

Shields, Erin; Krug, Jonathan; Linak, William; Jackson, Stephen; Roberson, William; Yamada, Takahiro; Kahandawala, Moshan

5d. PROJECT NUMBER
ER21-1288

5e. TASK NUMBER

5f. WORK UNIT NUMBER

7. PERFORMING ORGANIZATION NAME(S) AND ADDRESS(ES)

U.S. EPA Office of Research and Development
109 TW Alexander Dr
RTP, NC 27711
University of Dayton Research Institute
1700 S Patterson Blvd
Dayton, OH 45469

8. PERFORMING ORGANIZATION REPORT NUMBER

9. SPONSORING / MONITORING AGENCY NAME(S) AND ADDRESS(ES)

Office of the Deputy Assistant Secretary of Defense (Energy Resilience & Optimization)
3500 Defense Pentagon, RM 5C646
Washington, DC 20301-3500

10. SPONSOR/MONITOR'S ACRONYM(S)
SERDP

11. SPONSOR/MONITOR'S REPORT NUMBER(S)
ER21-1288

12. DISTRIBUTION / AVAILABILITY STATEMENT

DISTRIBUTION STATEMENT A. Approved for public release: distribution unlimited

13. SUPPLEMENTARY NOTES

14. ABSTRACT

The destruction of PFAS and PFAS-laden materials is a major area of importance for the EPA, DoD, States, and industries. It is necessary to ensure that PFAS are completely destroyed, i.e., mineralized, and not merely converted to other fluorinated compounds and released into the environment. The main objective of this research project is to improve the understanding of the fate of PFAS during thermal treatment, conditions needed for destruction, and to investigate alternative indicators of destruction to help verify PFAS destruction. Tests using C1 to C5 perfluorocarbons were performed in a bench-scale tube furnace and found that except for tetrafluoromethane the compounds were destroyed around 1000-1100°C, but some products of incomplete combustion were observed. A pilot-scale tunnel furnace was used to investigate the incineration of fluorocarbons, a legacy PFAS AFFF, and a fluorotelomer based AFFF. The results showed that as the temperatures approached 1100°C the PFAS were destroyed, and the products of incomplete destruction approached detection limits. Hexafluoroethane showed this type of trend too and could be a potential indicator to help evaluate PFAS destruction. These experiments were performed in simplified systems and matrices and may not directly apply to full-scale systems. This work helped establish methods to characterize emissions from incinerators to help determine if PFAS are mineralized during incineration. Future work should include pilot or full-scale systems burning typical hazardous waste streams to determine how mixed wastes and complicated matrices impacts PFAS destruction.

15. SUBJECT TERMS

PFAS, incineration, products of incomplete combustion, destruction, surrogate, AFFF, perfluorocarbons

16. SECURITY CLASSIFICATION OF: Unclass			**17. LIMITATION OF ABSTRACT**	**18. NUMBER OF PAGES**	**19a. NAME OF RESPONSIBLE PERSON**
a. REPORT	**b. ABSTRACT**	**c. THIS PAGE**	Unclass	69	Erin P. Shields
Unclass	Unclass	Unclass			**19b. TELEPHONE NUMBER** 919-541-3521

Standard Form 298 (Rev. 8-98)
Prescribed by ANSI Std. Z39.18

SERDP FINAL REPORT

Project: ER21-1288

TABLE OF CONTENTS

Page

TABLE OF CONTENTS (Continued)

Page

LIST OF FIGURES

Page

LIST OF TABLES

Page

ACRONYMS AND ABBREVIATIONS

AFFF	Aqueous film forming foam
APCS	Air pollution control system
AOF	Adsorbable organic fluorine
°C	Degrees Celsius
C# (C1, C2. . .)	Fluorinated carbon chain of # of carbons
C_2F_4	Tetrafluoroethylene
C_2F_6	Hexafluoroethane
C_3F_8	Perfluoropropane
C_4F_{10}	Perfluorobutane
C_5F_{12}	Perfluoropentane
CAS #	Chemical Abstracts Service number
CF_2O	Carbonyl difluoride
CF_4	Tetrafluoromethane
CLS	Classical least squares
CO	Carbon monoxide
CO_2	Carbon dioxide
DSCM	Dry standard cubic meter
DE	Destruction efficiency
DoD	Department of Defense
DRE	Destruction and removal efficiency
EPA	United States Environmental Protection Agency
FC	Fluorocarbon
FTAB	Fluorotelemer alkyl betaine
FTIR	Fourier transform infrared spectroscopy
FTS	Fluorotelomer sulfonate
GC/MS	Gas chromatography coupled with mass spectrometry
h	Hour
HF	Hydrofluoric acid
in	Inch
kJ/mol	Kilojoules per mole
kPa	kilopascal
kW	kilowatt
L/min	Liter per minute
LC/MS	High performance liquid chromatography coupled with mass spectrometry
M	Molar
ME	Mineralization efficiency
MFC	Mass flow controller
mg	Milligram
ng	Nanogram
ng/m^3	Nanograms per cubic meter
O_2	Oxygen
ORD	Office of Research and Development
OTM	Other Test Method
PFAS	Per- and polyfluoroalkyl substances

PFBA	Perfluorobutanoic acid
PFBS	Perfluorobutanesulfonic acid
PFC	Perfluorocarbon
PFHpA	Perfluoroheptanoic acid
PFHpS	Perfluoroheptanesulfonic acid
PFHxA	Perfluorohexanoic acid
PFHxS	Perfluorohexanesulfonic acid
PFOA	Perfluorooctanoic acid
PFOS	Perfluorooctanesulfonic acid
PFPeA	Perfluoropentanoic acid
PFPeS	Perfluoropentanesulfonic acid
PFCA	Perfluorocarboxylic acid
PFSA	Perfluorosulfonic acid
PICs	Products of incomplete combustion
PIDs	Products of incomplete destruction
ppb	Parts per billion
ppm	Parts per million
SERDP	Strategic Environmental Research and Development Program
SOP	Standard operating procedure
SR	Stoichiometric ratio
TOPA	Total oxidizable precursor assay
UDRI	University of Dayton Research Institute
VFC	Volatile fluorinated compound
$\mu g/m^3$	Micrograms per cubic meter

KEYWORDS

aqueous film forming foam (AFFF), incineration, mineralization, per- and polyfluoroalkyl substances (PFAS), products of incomplete combustion (PICs), surrogate, trial burn

ACKNOWLEDGEMENTS

We would like to acknowledge the methods development help that was provided by the previous SERDP project, ER19-1408, that had Jeffrey Ryan as the PI. Janice Willey, Billy Anderson, and Eurofins Environmental Testing are people outside of the EPA that helped lay the groundwork for OTM-45 and OTM-50.

Along with some of the authors, William Preston, of CSS Inc., helped develop OTM-50, a method to analyze volatile fluorinated compounds using evacuated canisters and GC/MS. This method was essential to this project.

Thank you to others that helped with this research. This includes EPA staff, Jeff Ryan, Libby Nessley, Ariel Wallace, C. W. Lee, Paul Lemieux, Larry Virtaranta, Peter Kariher, and Hannah Liberatore.

Environmental Protection Agency contract 68HERC20D0018 to Jacobs Engineering was used to help perform this project. Thank you to our on-site contractors with Jacobs Engineering, including Preston Burnette, Matt Allen, Stella McDonald, Katie Tyson, John Nash, Terrance Odom, and Neil Kinley.

Thank you to Diana Hanson and Robin Lundsford for your help with funds and contracts, too.

The bench scale research was carried out by University of Dayton Research Institute.

EPA research funds from the Sustainable and Healthy Communities National Research Program were also used for this project.

Disclaimers:

The views expressed in this SERDP report are those of the authors and do not necessarily represent the views or the policies of the U.S. Environmental Protection Agency.

Any mention of trade names, manufacturers or products does not imply an endorsement by the United States Government or the U.S. Environmental Protection Agency. EPA and its employees do not endorse any commercial products, services, or enterprises.

ABSTRACT

INTRODUCTION AND OBJECTIVES

The destruction of PFAS and PFAS-laden materials is a major area of importance for the EPA, DoD, States, and industries. It is necessary to ensure that PFAS are completely destroyed, i.e., mineralized, and not merely converted to other fluorinated compounds and released into the environment. This can be difficult to both accomplish and to verify that mineralization has occurred. To fully investigate this, it is important to determine what products of incomplete destruction are commonly formed and if a hard to destroy compound may be able to help indicate that PFAS mineralization is likely occurring. The main objective of this research project is to improve the understanding of the fate of PFAS during thermal treatment, conditions needed for destruction, and to investigate alternative indicators of destruction to help verify PFAS destruction.

TECHNICAL APPROACH

This work combined laboratory experiments and pilot-scale testing to begin to evaluate the effectiveness of thermal treatment for destruction of PFAS. PFAS thermal destruction was evaluated using neat perfluorocarbons and concentrated aqueous film forming foam (AFFF). Data from the work will be applied to determine if there may be an effective indicator compound to help determine a technology's PFAS mineralization efficacy. Lab-scale studies of thermal destruction mechanisms of various perfluorocarbons were used to determine the thermal destructibility of the compounds. The EPA's 64 kW pilot-scale furnace was used to investigate PFAS destruction, the common products of incomplete combustion (PICs) formed, and to determine effective indicator compounds for PFAS mineralization. The sampled destruction of the indicator compound and the destruction of PFAS in the furnace is the starting point for determining any correlation destruction of the perfluorocarbon and PFAS.

RESULTS

The bench and pilot scale studies with perfluorocarbons and two AFFFs have shown that common products of incomplete destruction include perfluorocarbons, 1H-perfluorocarbons, and perfluorocarboxylic acids. These compounds approach the detection limits, or blank levels, as the temperatures approach 1100 °C. The PFAS in both perfluorinated and fluorotelomer based AFFFs near the detection limit, or blank levels, in this same temperature range. The destruction of hexafluoroethane mirrors this destruction and absence of destruction byproducts. The use of hexafluoroethane, and in some instances tetrafluoromethane, shows promise as a potential destruction indicator compound for the mineralization of PFAS. This smaller scale research does not directly transfer to full scale systems but lays the groundwork for future full scale testing to determine if an indicator compound could be used to verify PFAS destruction.

BENEFITS

The accumulation of fundamental PFAS destruction data at various conditions and identifying potential indicator compounds to evaluate industrial-scale thermal treatment technologies will provide valuable information, practical evidence, and data for guidelines for PFAS destruction to transition to industry and DoD providers. The data and source evaluation procedure will give the DoD confidence that their PFAS wastes are being destroyed and potentially harmful PFAS by-products are not being released into the environment.

EXECUTIVE SUMMARY

INTRODUCTION

The unique chemical and physical properties of PFAS have led to their widespread use by the DoD and civilian industries. The strong carbon-fluorine bond and other unique properties make PFAS amenable to their use in many areas while creating a challenge for the removal and destruction of PFAS. One widespread use is in AFFF used by the DoD and civilian entities to extinguish fires, especially at airports, fuel terminals, chemical plants, and in enclosed spaces. The prevalent use of PFAS by industry and the DoD, and their very high environmental stability have contributed to their ubiquitous presence in soil, water, air, plants, animals, and humans globally. The many adverse health and environmental effects attributed to some PFAS have led to increased efforts to control releases and destroy PFAS-contaminated media. The DoD, governments, and industry are involved in research to remediate and destroy PFAS stockpiles, contaminated soils and water, and contaminated media used in remediation, however, there are few data showing what are the most effective technologies and conditions for complete destruction.

Both the influent waste stream and the emissions from a PFAS thermal treatment facility can be very complicated to analyze. A functional group on a parent PFAS can often be removed resulting in the formation of a volatile fluorinated compound (VFC) at relatively low temperatures. In flames and at high temperature, PFAS can break apart and recombine forming different and occasionally larger PFAS, and these molecules can inhibit combustion under incineration conditions as well. These thermal reactions/processes may form a variety of molecules such as non-polar highly volatile molecules like tetrafluoromethane, CF_4, and hexafluoroethane, C_2F_6, polar nonvolatile acids and alcohols upon oxidation in air or water, and possibly nonpolar semivolatile compounds too. The formation of fluorinated PICs with different properties from the parent molecule makes destruction and removal efficiencies (DREs) of PFAS an ineffective metric to evaluate PFAS destruction, including the determination of mineralization, i.e., the complete breaking of all the carbon-fluorine bonds to form hydrofluoric acid (HF) and carbon dioxide (CO_2). As a result, the comprehensive characterization of PICs is integral to assessing effective PFAS destruction. These changes and reactions that occur in thermal treatments makes data solely from targeting the starting material's targeted PFAS often misleading. Analyses looking for all types of PFAS and fluorochemicals need to be examined together to give the full picture of the PFAS destruction. The EPA applies its experience sampling and analyzing polar, non-polar, volatile, and nonvolatile samples to help identify targeted and nontargeted PICs and determine destruction of the parent molecules.

The variety of PFAS and the fluorinated compounds that can be formed as byproducts of their destruction makes it hard to determine the extent of the parent PFAS' mineralization. The use of a more stable and easily measured compound that could be used to indicate how well PFAS are being destroyed could provide a more complete determination of mineralization. With enough data to help correlate a compound, like hexafluoroethane or other perfluorocarbon (PFC) with PIC formation, the indicator compound could be used like traditional surrogate compounds to help establish a facility's operating parameters to properly destroy PFAS. Alternative indicators, sometimes referred to as "surrogates" are often used for hazardous wastes that are dangerous or difficult to destroy, so industry and regulators are used to using them for trial burns. C_2F_6 and CF_4 are currently used to help assess the destruction efficiencies for greenhouse gas destruction technologies, so considering alternative indicators for assessing complete PFAS thermal

destruction may be applicable if a relationship between alternative indicator destruction and overall PFAS complete destruction can be established.

This project's central hypothesis was that thermal studies and alternative indicator testing will provide a fundamental understanding of PFAS destruction mechanisms and requirements for the complete destruction of PFAS. Each furnace and thermal treatment facility is different and may require different parameters to mineralize PFAS, so this project aims to define a process for stakeholders to help determine parameters for the mineralization of PFAS. The objective includes identifying and minimizing PICs during the processes. The use of indicator compounds, for a potential surrogate, will be investigated to determine if full scale testing of the compound is promising. This effort will enable the thermal destruction of PFAS to be more thoroughly understood, provide methodologies to evaluate industrial thermal treatment facilities, and will inform what conditions may be needed to fully destroy PFAS.

To investigate the thermal destruction of PFAS and potential indicator compounds, both bench scale and pilot scale testing were used. Perfluorocarbons, trifluoromethane, and AFFF concentrate were incinerated, and the emissions characterized to determine the parent compounds destruction, PICs formed, and to look for any correlation with the destruction of the alternative indicator compounds.

OBJECTIVES

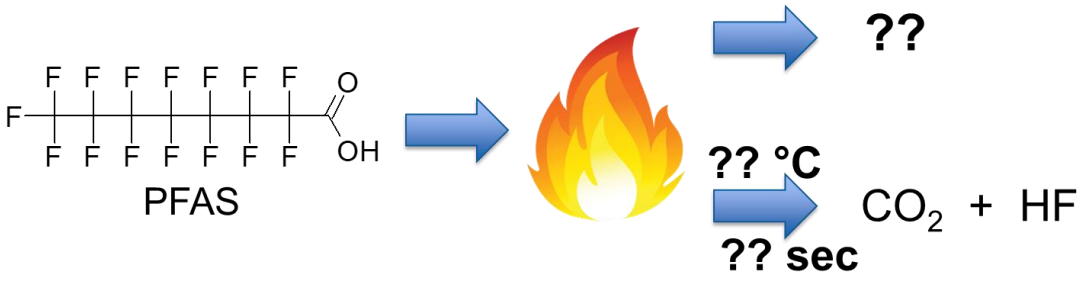

Figure ES 1. The aim of this project is to find what is formed with incomplete destruction and how to determine if the conditions are met for mineralization

The main objective of this research project is to improve the understanding of the fate of PFAS during thermal treatment and to investigate alternative indicators of destruction (surrogates) to help verify the destruction of PFAS. This will be developed through answering the following questions:

- What are the conditions needed for PFAS destruction?
- Are all the carbon-fluorine bonds destroyed at standard incinerator temperatures, or are fluorinated PICs formed?
- Can molecules be destroyed thermally or are flame-produced free radicals necessary for reaction?
- Can a surrogate molecule represent PFAS of concern to aid in the determination of the efficacy of a thermal treatment technology?

TECHNOLOGY APPROACH

The project consisted of experiments at benchtop scale, up to about 8 L/min flow, and at pilot scale, about 1000 L/min flow rate. The bench scale experiments investigated PFC destruction and the pilot scale system was used to study fluorocarbons (FCs) and two AFFF concentrates. The approach to the experiments is briefly state here.

The benchtop study was conducted using two tube furnaces, one for temperatures up to 1150 °C and on for temperatures up to 1600 °C, with the same setup as shown in Figure ES 2. C1 to C5 PFCs were fed into the furnaces with humidified air or nitrogen carrier gases. The carrier gas flow rate was changed to vary the residence times in the high temperature zones, from 2 to 8 s. For CF_4 the high temperature furnace was used to test at 1300, 1450, and 1600 °C, while the other gases were tested at 850, 1000, and 1150 °C in the lower temperature furnace. The emissions were analyzed by Fourier transform infrared spectroscopy (FTIR) and by measuring the fluoride ions collected in impingers.

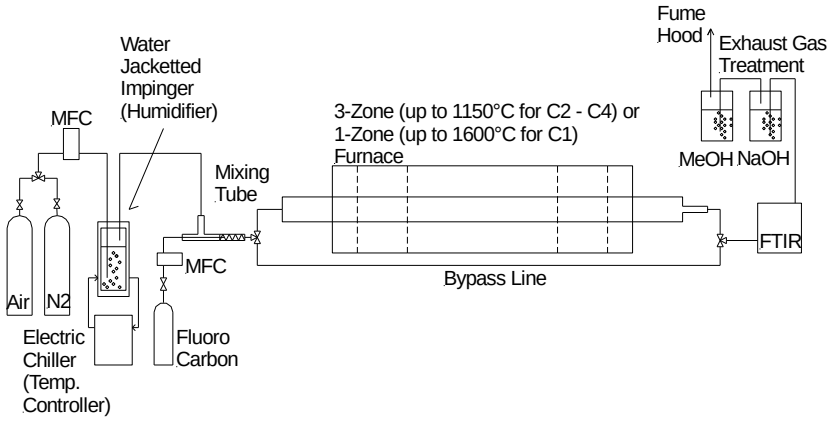

Figure ES 2. Tube furnace setup for bench scale experiments

The pilot scale experiments were conducted on the EPA ORD's 64 kW down fired tunnel furnace, see Figure ES 3. This furnace is similar to a thermal oxidizer. The liquids or gases to be incinerated can be injected through the flame in the combustion air or the natural gas or through ports located along the straight zone after the flame. The temperatures were controlled by varying the amount of natural gas burned and by injecting the samples at ports along the side. The combustion air flow was changed to at each firing rate to keep the flow rate of the furnace at about 1000 L/min.

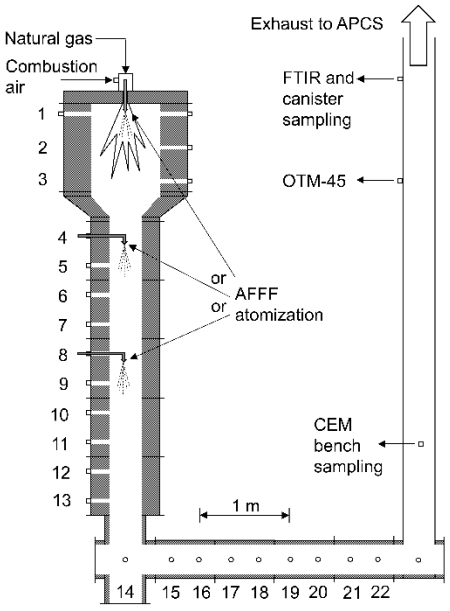

Figure ES 3. Pilot scale furnace schematic.

Sampling was done using FTIR both alone and with other test method (OTM)-45, OTM-50, and Method 0010. The OTM-45 and OTM-50 trains were analyzed according to the most recent version of the method at the time of analysis. The Method 0010 trains were extracted using Method 3542 and analyzed following Method 8270.

Samples were injected into the furnace in different ways, attempting to mimic commercial injection techniques. To minimize HF formation that may harm the ductwork after the sampling locations, the FC gases were limited to about 35 mL/min injection rate, and the AFFFs were kept between 13 and 14 g/min. The FC gases and AFFF were injected through the flame using a burner with an atomizing tube down the center. Initial tests with the FCs used a quartz tube to inject the neat gases. The legacy AFFF was injected using a dual fluid atomizer that was air cooled. This introduced up to 50 L/min excess air and could impact the flow rate. The fluorotelomer AFFF and C_2F_6 were injected with a water-cooled dual air atomizer that only added 10 L/min.

The temperature ranges for injection of AFFFs and FCs into the side of the pilot scale tests ranged from 760 to 1180 °C, and the legacy AFFF and FCs were also injected through the flame. Typically, ports 4, 6, and 8 were used. Port 10 was used sparingly due to its proximity with the 90° angle.

RESULTS AND DISCUSSION

The bench scale experiments investigated the destruction and mineralization of PFCs from tetrafluoromethane to dodecafluoropentane (C1 to C5). The atmosphere was changed between air and nitrogen to study the effect of excess O_2 and pyrolytic conditions. FTIR was used to calculate the destruction of the PFC and to look for PICs that may be amenable to FTIR.

For all the PFCs the common PICs were carbonyl difluoride (CF_2O), trifluoromethane (CF_3H), and tetrafluorosilane (SiF_4, from reactions with the quartz tubes). Occasionally, C_2F_6 was observed. These PICs were more prevalent with the nitrogen atmosphere than with oxygen present. CF_3H was typically not present once the temperature exceeded 1000 °C, while CF_2O was seen in most every run and temperature.

The compounds measured by FTIR and the PFC destruction efficiency (DE) and the mineralization efficiency (ME) in air at 1000 °C are listed in Table ES 1. The ME was estimated by dividing the free fluorine by the total amount of the fluorine added. SiF_4 was included since it is formed primarily from HF reacting with the quartz surfaces. Reactions with surfaces negatively impacts ME, so ME is not as reliable mineralization metric as determining the presence of PICs. The longer chain PFCs were destroyed at about the same temperature as C_2F_6 but required higher temperatures or longer residence times to reduce most of the PICs to nondetect levels. CF_2O persisted though. The C3 – C5 chains stayed showed more PICs even with high DEs. This indicates that PFC chains longer that C2, may not be effective surrogates since they produce more PICs.

Table ES 1. FTIR measurements of C2 to C5 perfluorocarbons in air at 1000 °C and 2 s

Compound	C_2F_6	C_3F_8	C_4F_{10}	C_5F_{12}
Res. Time (s)	2	2	2	2
Bypass conc. (ppm)	119.6	111.5	115.0	123.1
Detected conc. (ppm)	9.06	0.0	0.0	0.0
HF (ppm)	285.2	336.8	376.4	504.3
CF_2O (ppm)	164.1	305.3	404.5	186.7
SiF_4 (ppm)	0.0	0.5	1.1	1.7
CF_3H (ppm)	0.0	0.0	0.0	1.9
DE (%)	92.4	>99.9	>99.9	>99.9
ME (%)	39.7	38.0	33.1	34.6

Pilot scale tests with C1 and C2 FCs showed similar results to the bench sale tests. CF_4 was the most difficult to destroy compound that could still survive flame conditions. Some PICs were observed with the FTIR, CF_4 and C_2F_6. CF_2O was not confirmed as a PIC, likely due to the high concentrations of water due to the natural gas combustion (~11 – 15%). A summary of the FC destruction is shown in Table ES 2. C_2F_6 looks to be a promising candidate for a surrogate compound, since it has a destruction profile from around 900 to 1100 °C.

Injecting a perfluorinated legacy AFFF helped determine what types of PICs may be formed and helped give a rough estimate of where the concentrations of PICs are near the detection limit and there was high destruction of the PFAS in the AFFF. The data is summarized in Table ES 3. The conditions that produced low PICs and high DEs for the PFAS also show high destruction of C_2F_6. This is promising for the use of C_2F_6 as a potential indicator compound or surrogate.

Table ES 3 shows that even if the PFAS has high DEs, mineralization may not be occuring. There are volatile fluorinated compounds (VFCs) PICs measured by OTM-50 even when the DE of the PFAS is over 99.9%. This helps verify that DE alone is not a good metric for PFAS destruction.

Table ES 2. Fluorocarbon destruction in the pilot scale furnace

Temperature (°C)	DE (%)		
	CF_4	CHF_3	C_2F_6
Combustion air	88.7	>99	>99
Natural gas	94.9	>99	>99
1295	13.7	>99	>99
1203	12.9	>99	>99
1127	11.7	>99	>99
1090	-	>99	>99
1060	12.5	>99	>99
984	-	>99	86.2
960	-	-	78.2
930	-	>99	25.5
830	-	94.3	0

Table ES 3. Legacy AFFF destruction, PICs, and comparison to C_2F_6 destruction

Temperature (°C)	FTIR		Targeted PFAS			
	Initial C_2F_6 (ppmv)	C_2F_6 (ppmv)	Initial PFAS (g/m^3)	OTM-45 (ng/m^3)	OTM-45 %DE	OTM-50 ($\mu g/m^3$)
Flame	34	<0.0005	973	38.0	99.9994	1.1
1180	33	<0.0005	796	200	99.9964	1.2
1090	32	5.71	792	74.7	99.9995	3.2
970	33	24.5	791	636	99.9814	294.7
870	33	27.1	796	2950	99.8160	2460
810	33	28.8	798	173000	92.9512	26540

To study what PICs can be formed from the thermal treatment of various AFFFs, a fluorotelomer AFFF was tested too. This AFFF was injected post-flame from 760 to 1180 °C. This AFFF contained low double digit ppm concentrations of targeted PFAS but literature states the AFFF should contain about 7000 ppm of PFAS. The fluorotelomer based AFFF exhibited about the same results as the legacy AFFF. Both AFFF types had the same common PICs: PFCs, 1H-perfluorocarbons, and perfluorocarboxylic acids. With high destruction of the targeted PFAS and low concentrations of PICs occuring as the temperature approached 1100 °C, see Tables ES 4. Again, C_2F_6 showed high destruction when there were few PICs and high DEs for the PFAS, as shown in Table 4 for the co-injection of C_2F_6 with the AFFF. The injection of the C_2F_6 did produce a low concentration of CF_4 as a PIC at the higher temperatures.

Table ES 4. Summary of fluorinated emissions from the incineration of fluorotelomer AFFF and a comparison of the destruction of C_2F_6

Temperature (°C)	760	860	880	1010	1080	1160
Injection Port	**8**	**4**	**8**	**8**	**6**	**4**
Total PFAS – OTM-45 (ng/m^3)	25260	28.1	243.1	30.8	16.1	14.7
Total VFCs – OTM-50 ($\mu g/m^3$)	1951	105.83	125.77	17.31	3.98	0.55
C_2F_6 DE (%)	-	41.46	6.87	96.64	99.93	99.98

These studies verified that the DE of the original PFAS should not be the only metric used to determine the efficacy of destruction technologies. The emissions need to be characterized for nonpolar and polar fluorinated PICs. This shows the value of an indicator compound (like C_2F_6) to help evaluate the system and to help develop a correlation with PFAS destruction and the presence of PICs.

IMPLICATIONS FOR FUTURE RESEARCH AND BENEFITS

The accumulation of fundamental PFAS destruction data and identifying an effective indicator compound to evaluate industrial-scale thermal treatment technologies will provide valuable information, practical evidence, and data for guidelines for PFAS destruction to transition to industry and DoD providers. The data and source evaluation procedure will give the DoD

confidence that their PFAS wastes are being destroyed and potentially harmful PFAS by-products are not being released into the environment.

The research performed here with the benchtop and pilot-scale systems provides insight to the objectives of this project and provide insight into the incineration of PFAS. Here, it was observed that conditions with temperatures approaching 1100 °C can destroy PFAS and produce limited PICs. The availability of radicals from flames of other compounds can help increase the destruction of PFAS too. High destruction of the original PFAS can occur, but there can be PICs formed such as fluorocarbons or shorter chain carboxylic acids. Hexafluoroethane and to some degree tetrafluoromethane have destruction profiles that correlate to the presence of PICs and may be helpful to provide an indication of an incinerator's performance and may be potential surrogate candidates. Ultimately, these results are specific to the systems used for this study and more research is needed to understand if these results apply to real-world full-scale systems. These results do show that the incineration of PFAS may be a promising method to destroy PFAS, and that further research is worthwhile. Also, the methods developed for characterization the PFAS in the emissions can provide an effective way to evaluate full-scale systems.

This project was performed at a pilot scale incinerator that is closer to a thermal oxidizer than most commercial incineration facilities. The results here may not translate directly to full-scale hazardous waste incinerators. Commercial incinerators have complicated feeds, varying time and temperature profiles, possible cold or hot zones, and other aspects that may aid or hinder PFAS destruction. It is vital to perform similar source emissions characterizations and indicator injections at full scale facilities. This would involve the facility burning their typical waste stream along with the PFAS laden material. These full-scale tests would help determine if any correlation between indicator gases and the presence of PICs that was observed with the simple AFFF matrix here, would carry over to real-world incinerators.

Full-scale real-world testing or even further pilot-scale tests, need to investigate the emissions from the incineration a typical feed of hazardous waste, e.g., chlorinated and other halogenated wastes, organic solvents, soil, solid waste, and other materials, with the PFAS. Chlorinated and brominated wastes are known to aid in the molecular growth of PICs and produce highly toxic species such as chlorinated dioxins and PCBs. It is important to verify if mixed fluorinate and hazardous wastes produce any similar products, or if the fluorine enhances the formation of nonfluorinated compounds of concern.

1.0 OBJECTIVE

The Strategic Environmental Research and Development Program's (SERDP) Environmental Restoration program statement of need, ERSON-21-C1, identified the need for improved understanding of the thermal destruction of per- and polyfluoroalkyl substances (PFAS). This included a desire to learn what products of incomplete combustion (PICs), or products of incomplete destruction (PIDs), may be formed and what temperatures may result in the mineralization of PFAS, as depicted in Figure 1. Incineration and thermal treatment are readily available technologies that can treat large amounts of waste, so this information is vital to determine if thermal treatment is a viable method to treat PFAS contaminated waste streams.

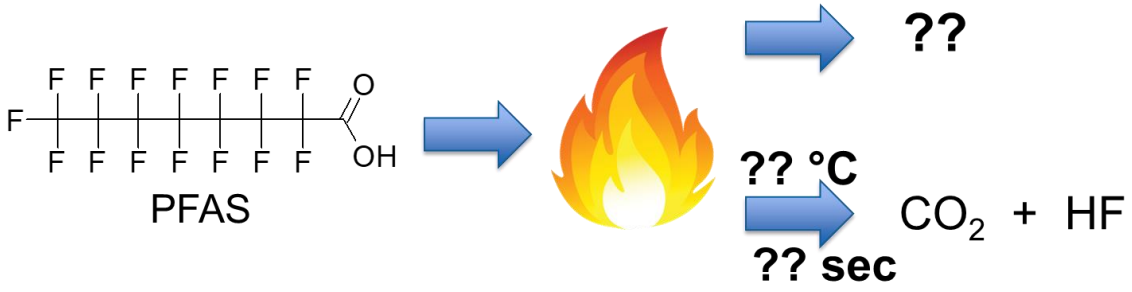

Figure 1. Overview of research objectives. What can form with incomplete combustion and how can it be determined what conditions are needed for mineralization.

The main objective of this research project is to improve the understanding of the fate of PFAS during thermal treatment and to investigate alternative indicators of destruction (surrogates) to help verify the destruction of PFAS. This will be developed through answering the following questions:

- What are the temperature requirements for PFAS destruction?
- Are all the carbon-fluorine bonds destroyed at standard incinerator temperatures, or are fluorinated PICs formed?
- Can molecules be destroyed thermally or are flame-produced free radicals necessary for reaction?
- Can a surrogate molecule be used to simplify the determination of the efficacy of a thermal treatment technology?

2.0 BACKGROUND

The unique chemical and physical properties of PFAS have led to their widespread use by the DoD and civilian industries. The strong carbon-fluorine bond and other unique properties make PFAS amenable to their use in many areas while creating a challenge for the removal and destruction of PFAS. One widespread use is in AFFF used by the DoD and civilian entities to extinguish fires, especially at airports, fuel terminals, chemical plants, and in enclosed spaces. The prevalent use of PFAS by industry and the DoD, and their very high environmental stability have contributed to their ubiquitous presence in soil,[1, 2] water,[3] air,[1] plants,[2] animals,[4] and humans[3, 5] globally. The many adverse health and environmental effects attributed to some PFAS[2-4] have led to increased efforts to control releases and destroy PFAS-contaminated media. The DoD, governments, and industry are involved in research to remediate and destroy PFAS stockpiles, contaminated soils and water, and contaminated media used in remediation, however, there are few data showing what are the most effective technologies and conditions for complete destruction.

The carbon-fluorine bond is the strongest carbon single bond, with bond dissociation energies up to 544 kJ/mol in tetrafluoromethane, CF_4.[6] The temperatures required to break these bonds can reach up to 1600 °C.[7] Even using plasma with temperatures over 1500 °C, longer chain perfluorocarbons still produce smaller fluorocarbons (FCs) that have been detected in the exhaust stream.[8] These products of incomplete combustion (PICs), or products of incomplete destruction (PIDs), may still have detrimental environmental and health effects, are often be more volatile than the parent compound, and can transform to other PFAS in the environment.[1, 9-11] It is important to determine what PIDs are formed and emitted when using thermal treatment processes and other destruction technologies. Chemical characterization of the PIDs formed, if any, will provide valuable information for determining and designing effective treatment technologies and controls for the remediation of media, soils, and waters contaminated by PFAS.

Incineration has been used for decades to destroy hazardous wastes and may offer a readily available full scale solution to treating concentrated PFAS waste streams, like AFFF. Besides the established incinerators, thermal treatment technologies for the remediation of AFFF contaminated soils are being developed by several groups under the SERDP program. EA Engineering, Science, and Technology performed a desorption and thermal oxidation test that effectively removed AFFF from sand (ER18-1572). A group from CH2M Hill used infrared heat to desorb the AFFF in soils (ER18-1603). An ex- and in-situ smoldering combustion approach for PFAS contaminated soils and GAC was developed by Geosyntec (ER18-1593). Low temperature thermal degradation of PFAS aided by calcium hydroxide is being explored further by APTIM Federal Services (ER18-1556). These techniques provide promising results but the fundamental processes and characterization of PICs for the desorption or destruction steps have not been completely evaluated. The most significant impediment to this evaluation is the development of air sampling and analytical methods, as the current state of the science for soil and water analysis is significantly more advanced than that for emissions. In part this is due to the advances made in past and on-going SERDP-sponsored analytical methods research on PFAS in soil and water. Dr. Slater (ER19-1128), Dr. Liu (ER-1157), Dr. Peaslee (ER19-1142), and Dr. Hanigan (ER19-1214) all are developing methods for soil and water analysis. There remains a gap in the characterization of emissions from thermal treatment technologies resulting in uncertainty about PFAS destruction requirements. This gap is largely due to a lack of sampling and analytical methods being available. Recently, the EPA, with help from SERDP project ER19-1408, has released two Other Test

Methods to help address this analytical gap.[12, 13] Now both PFAS and volatile fluorinated compounds (VFCs) can be measured in emissions, but there is little to no data to characterize the emissions from thermal treatment sources and determine their efficacies.

Both the influent waste stream and the emissions from a PFAS thermal treatment facility can be very complicated to analyze. A functional group on a parent PFAS molecule can often be removed to form a volatile VFC at relatively low temperatures.[9, 10, 14] In flames and at high temperature PFAS can break apart and recombine forming different and occasionally larger PFAS,[11, 15, 16] and these molecules can inhibit combustion under incineration conditions as well. These thermal reactions/processes can produce a variety of molecules such as non-polar highly volatile molecules like hexafluoroethane, C_2F_6, nonpolar semivolatile compounds, and polar nonvolatile acids and alcohols. The formation of fluorinated PICs with different properties from the parent molecule makes destruction and removal efficiencies (DREs) of PFAS an ineffective metric to evaluate PFAS destruction and determine mineralization, or the breaking of all the carbon-fluorine bonds to form hydrofluoric acid (HF) and carbon dioxide (CO_2). These changes and reactions that occur in thermal treatments makes data solely from targeting the starting material's targeted PFAS often misleading. Analyses looking for all types of PFAS and fluorochemicals need to be examined together to give the full picture of the PFAS destruction. The EPA applied its experience sampling and analyzing polar, non-polar, volatile, and nonvolatile samples to help identify targeted and nontargeted PFAS[17, 18] PICs and determine destruction of the parent molecules.

The variety of PFAS and the fluorinated compounds that can be formed as byproducts of their destruction makes it hard to determine the extent of the parent PFAS' mineralization. The use of a more stable and easily measured compound that could be used to indicate how well PFAS are being destroyed would make determining the technology's efficacy easier. Alternative indicators, sometimes referred to as "surrogates" are often used for hazardous wastes that are dangerous or difficult to destroy, so industry and regulators are used to using them for trial burns. With enough data to help correlate a compound, like hexafluoroethane or other perfluorocarbon, the indicator compound could be used like traditional surrogate compounds to help establish a facility's operating parameters to properly destroy PFAS. Surrogate methods are often used for hazardous wastes that are dangerous or difficult to destroy,[19, 20] so industry and regulators are used to using them for trial burns. C_2F_6 is currently used to help determine the destruction efficiencies for greenhouse gas destruction technologies,[21] so C_2F_6's use is not new either.

This project's central hypothesis was that thermal studies and the use of alternative indicators testing can help provide a fundamental understanding of PFAS destruction and requirements for the complete destruction of PFAS. Each furnace and thermal treatment facility is different and may require different parameters to mineralize PFAS, so this project aimed to define a process for stakeholders to help determine parameters for the mineralization of PFAS. The objective included identifying and minimizing PICs during the processes. The use of indicator compounds, for a potential surrogate, was investigated to determine if full scale testing of the indicators is promising. This effort provided data and helped establish a framework for the thermal destruction of PFAS to be more thoroughly understood, provided methodologies to evaluate industrial thermal treatment facilities, and helped provide best case conditions that may be needed to fully destroy PFAS.

To investigate the thermal destruction of PFAS and potential indicator compounds, both bench scale and pilot scale testing were used. Perfluorocarbons, trifluoromethane, and AFFF

concentrate were incinerated, and the emissions characterized to determine the parent compounds destruction, PICs formed, and to look for any correlation with the destruction of indicator gases.

3.0 MATERIALS AND METHODS

3.1 BENCH SCALE PERFLUOROCARBON THERMAL DESTRUCTION

Figure 2 shows the schematics of the bench scale PFC thermal destruction system used for the study. The thermal destruction of five PFCs listed in Table 1 was investigated using high- and medium-temperature furnaces (H18-40HTC, MHI and SST-3.00-0-30-3C-D2155-8E, Thermcraft) that can heat up to 1,600 and 1150°C, respectively.

The reactor used for high- and medium-temperature furnaces were 35mm x 42mm ID x OD, 40" length alumina and 47mm x 50 mm ID x OF, 52" length fused silica quartz tube reactors, respectively. CF_4 was thermally stable; therefore, a high temperature furnace was necessary to achieve high levels of destruction. The system was comprised of an air and nitrogen (N_2) supply controlled by a mass flow controller (MFC) (601FX, Porter). The MFC was calibrated by an ISO 17025 accredited calibration service company prior to the testing. The calibrated MFC (MCWM-5SCCD-D, Alicat) was also used to introduce PFCs into the reactor. The Air and N_2 were first passed through a humidifier to supply the hydrogen source to convert liberated fluorine to HF. The humidifier temperature was set at 15 °C controlled by the electric chiller (DC-0506, Water Bath). It gives a moisture concentration of 1.7%. The effluent gas was analyzed in situ using a Fourier transform infrared spectrometer (FTIR, MultiGas 2030, MKS). The FTIR was setup and used according to the procedures outlined in Appendix C.1. Conservative detection limits of 0.1 ppm were used for non detects, as 100 ppb is the highest detection limit provided by the manufacturer. Prior to performing destruction experiments, an axial reactor temperature profile was measured using a calibrated NIST traceable thermocouple (T5R-015-30 and KMQXL-125U-48, Omega Engineering) and thermocouple reader (CL23A and CL3515R, Omega Engineering). Prior to conducting PFC thermal treatment for each compound, helium was flowed through the system and a gas leak check was performed using a helium leak detector (Leak Detector 28500, Restek).

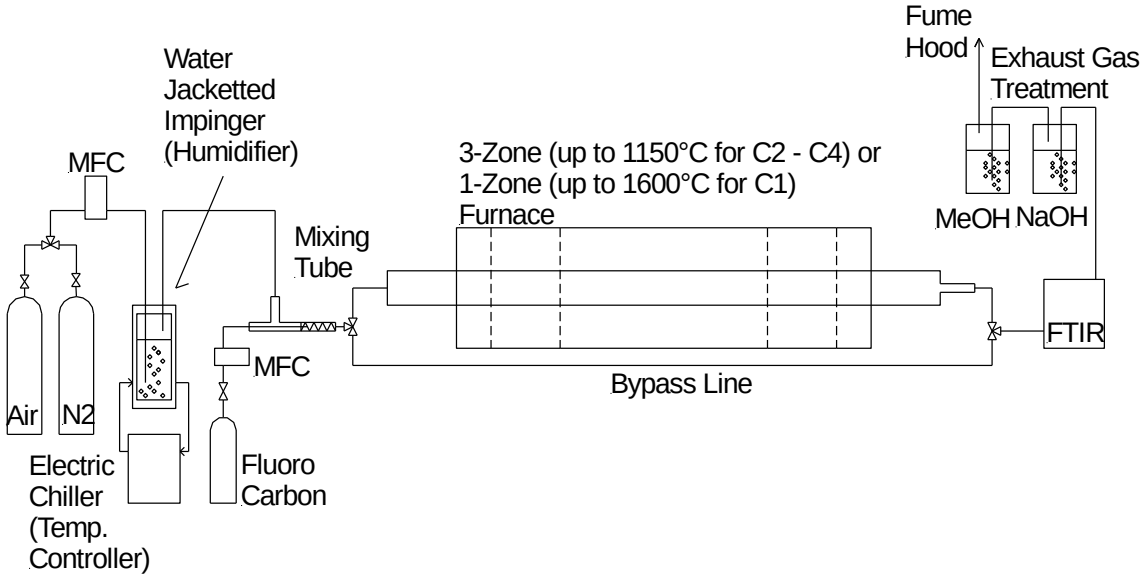

Figure 2. Schematic of the bench scale system used for perfluorocarbon experiments

Table 1. Perfluorocarbons incinerated in the bench scale furnace

Compound	Formula	CAS #
Tetrafluoromethane	CF_4	75-73-0
Hexafluoroethane	C_2F_6	76-16-4
Octafluoropropane	C_3F_8	76-19-7
Decafluorobutane	C_4F_{10}	355-25-9
Dodecafluoropentane	C_5F_{12}	678-26-2

The conditions set for the high temperature furnace is shown in Table 2, and the medium temperature furnace's conditions are shown in Table 3. The heating zone length was determined by the length that had temperatures within 5% of the highest measured temperature. The residence times were set by changing the flow rates of the carrier gases.

Table 2. High temperature tube furnace operating parameters

Targeted Temperature (°C)	1300		1450		1600	
Air Flow Rate (L/min)	1.225	0.612	1.225	0.612	1.225	0.612
Effective Length (in)	10	9.5	10	10.5	10.5	10.5
Average Temperature (°C)	1292	1298	1439	1434	1584	1581
Residence Time (s)	2.2	4.2	2.0	4.3	2.0	3.9

Table 3. Medium temperature tube furnace operating parameters

Targeted Temperature (°C)	850				1,000				1,150			
Air Flow Rate (L/min)	2	4	6	8	2	4	6	8	2	4	6	8
Effective Length (in)	27	27	27	27	28	28	27	27	29	29	28	29
Average Temperature (°C)	853	848	847	846	1005	1003	1002	1000	1148	1145	1146	1143
Residence Time (s)	9.4	4.5	3.0	2.3	8.3	4.1	2.7	2.0	7.4	3.8	2.5	1.9

3.2 PILOT SCALE FLUOROCARBON THERMAL DESTRUCTION

3.2.1 Experimental furnace

The pilot scale FC experiments performed using the Rainbow furnace (Figure 3) located at the EPA's Research Triangle Park location have been described previously.[22] This research combustor was designed to simulate the time-temperature and mixing characteristics of practical industrial liquid waste incineration systems and is described in greater detail in literature.[22, 23] All measurements reported were collected by a probe through Port 18 (Figure 3) before the effluent enters a facility air pollution control system (APCS). Since particulate and acid gas controls are not included, we report DEs rather than DREs. For these experiments, natural gas and combustion air were introduced into the combustor separately through an International Flame Research Foundation (IFRF) moveable-block variable air swirl burner. Excess air was maintained at 20%

(stoichiometric ratio, SR=1.2), and burner swirl was set at 4, midway on the 0-8 scale. Natural gas and combustion air were measured with two mass flow meters (Kurz Instruments Inc., models 504FT-12 and 504FT-32, respectively, Monterey, CA). The natural gas flow was controlled by a mass flow controller (Alicat model MCRW, Tucson, AZ) and the combustion air adjusted manually using a variable frequency drive to control the speed of the blower. Furnace load (fuel consumption) was used to vary peak furnace temperatures. Furnace loads of 40, 45, and 64 kW were used to provide a temperature range from 830 – 1280 °C for most FCs, within the range of most commercial incinerators and hazardous waste incinerators (HWIs). The 64 kW load was used for the injecting CF_4 into a flame with temperatures around 1600 °C. Temperature measurements were performed at 45 kW load using a suction pyrometer with a ceramic shielded thermocouple (Omega, model Type R, Norwalk, CT) located at the furnace centerline. A residence time profile was calculated using input flow rates, discretizing the Rainbow furnace volume between ports, and calculating temperature-corrected volumetric flow rates and residence times for each section. Incremental residence times were then summed along the length of the furnace. Ceramic shielded non-suction pyrometer thermocouple (Omega, model Type R, Norwalk, CT) temperature measurements were also performed at 40, 45, and 64 kW (20% excess air) during FC experiments. A combination of FTIR (MKS Instruments Inc., model 2030, Andover, MA) and a continuous emission monitor (CEM, California Analytical, model ZRE Analyzer, Orange, CA) measured furnace exhaust concentrations of oxygen (O_2), carbon monoxide (CO), and carbon dioxide (CO_2). These measurements are intended to verify combustion conditions and quantify small amounts of air leakage caused by the facility's induced draft blower.

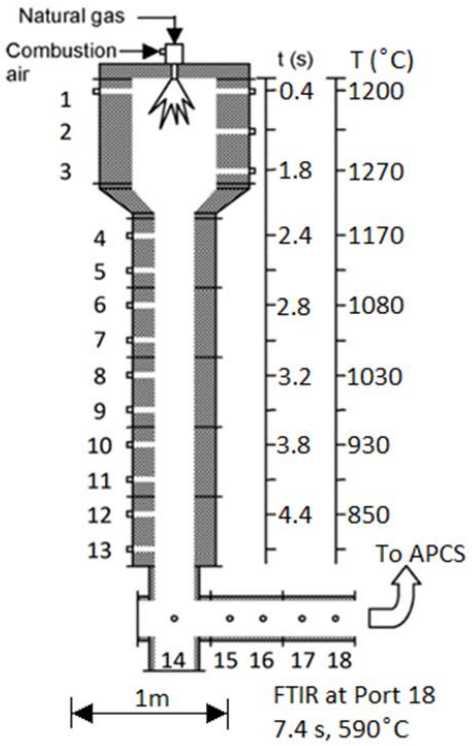

Figure 3. EPA's pilot-scale "Rainbow" research furnace with temperature and calculated residence time profiles at 45 kW natural gas, 20% excess air used for model conditions. FTIR samples collected at Port 18. Note the 1 m length scale.

3.2.2 Fluorocarbon injection experiments

FC destruction experiments were conducted by introduction of CF_4, CHF_3, or C_2F_6, using a mass flow controller (Sierra Instruments, model Smart Trak C100-L, Monterey, CA). The FCs were added to the natural gas or combustion air immediately before the burner, or axially through furnace ports at post-flame locations using a ¼" quartz tube. The FTIR continuously extracted gases from a fixed location (Port 18 shown in Figure 3) provided continuous spectral data that could be used to simultaneously quantify emission concentrations of the three FCs, limited fluorinated PICs, HF, and additional non-fluorinated species. From the FTIR library of compounds' reference spectra and calibrations, a subset recipe list of analytes was created. The specific recipe of compounds established for these measurements is presented in Table 4. The FTIR system consisted of a heated probe and filter for particulate removal and gas distribution, a heated sample line, and a heated pump for sample delivery. All heated components were maintained at 180 °C (356 °F) while the FTIR was maintained at 191 °C (376 °F). Measurements were informed by EPA Method 320 (Vapor Phase Organic and Inorganic by Extractive FTIR) (U.S. EPA, 2019) and ASTM D6348-12 (Standard Test Method for Determination of Gaseous Compounds by Extractive Direct Interface Fourier Transform Infrared (FTIR) Spectroscopy) (ASTM, 2012) as the primary approach. Reference gases containing known concentrations of CF_4, CHF_3, and C_2F_6 were used to confirm measurement data quality. These gases were injected directly to the FTIR to verify FTIR reference spectra accuracy. These gases were also injected at the probe through the entire FTIR sampling system using dynamic spiking, a form of standard addition, to assess overall measurement quality and measurement sensitivity. To determine emission concentrations, experimental conditions were established, and once the FTIR achieved a steady state, one-minute readings over five minutes were averaged. FTIR spectral residuals were calculated by classical least squares (CLS) in the MKS MG2000 software. If an unknown gas was present, then the CLS regression will have a poor fit with the adsorption spectrum of the unknown being shown in the residual. In this way, the residual acts as a built-in quality control feature to indicate interference or the presence of an unknown absorbance in the same wavelength spectrum. The residuals were averaged and compared to the FTIR target analyte concentration averages. Concentrations that were greater than 3x the residuals were considered a "real" result. The wet-basis concentration was used for the results.

Table 4. Compounds in FTIR Recipe

Fluorinated species		Non-fluorinated species	
Difluoromethane	CH_2F_2	Carbon dioxide	CO_2
Carbon tetrafluoride	CF_4	Carbon monoxide	CO
Carbonyl fluoride	CF_2O	Ethane	C_2H_6
Fluoromethane	CH_3F	Ethylene	C_2H_4
Hexafluoroethane	C_2F_6	Formaldehyde	CH_2O
Hydrogen fluoride	HF	Methane	CH_4
Sulfur hexafluoride	SF_6	Nitric oxide	NO
Trifluoromethane	CHF_3	Nitrogen dioxide	NO_2
		Nitrous oxide	N_2O
		Water	H_2O

3.3 PILOT SCALE LEGACY AFFF COMBUSTION

3.3.1 Experimental furnace

The pilot-scale furnace and burner described in section 3.2.1 and elsewhere[22, 24, 25] were used here. Here the furnace load and flame stoichiometric ratio (SR) were varied between 30-45 kW, and 1.3-2.0, respectively. To provide similar mass flows and thorough mixing of the effluent, high amounts of excess air were used to reduce and vary furnace temperatures to those more typical of HWIs and other incineration systems. Figure 4 presents a cutaway drawing of the Rainbow furnace with AFFF injection locations (burner, port 4, port 8) and stack sampling locations identified.

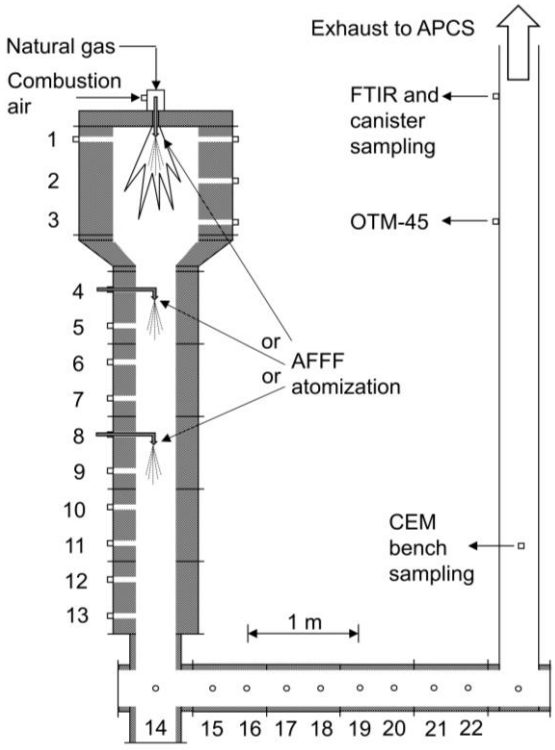

Figure 4. EPA refractory-lined natural gas-fired furnace showing the AFFF injection locations, through the flame with the natural gas and at ports 4 and 8 and the stack sampling locations indicated. Measurements are made prior to the facility APCS.

The Rainbow furnace operating conditions for each injection experiment were varied to produce varied temperatures for the experiments. The conditions are listed in Table 5. Rainbow furnace temperatures included one flame experiment where the AFFF would be exposed to near adiabatic flame temperatures (1963 °C for a methane-air diffusion flame at 101 kPa) and free radical chemistry characteristic of a natural gas diffusion flame, and five post-flame experiments that varied the peak (injection) temperature from 1180 to 810 °C in approximate increments of 100 °C.

Table 5. Furnace conditions for each temperature condition

Furnace setting, firing rate, FR	Thermal load, kW	Stoich. ratio, SR	NG flow rate, L/min	Air flow rate, L/min	Injection location	Port temperature[1], °C	AFFF feed rate, mL/min	Atomizing air flow rate, L/min	Injector sweep air 1 flow rate[2], L/min	Injector sweep air 2 flow rate[2], L/min	AFFF feed rate, g/min
1	30	2.0	48.7	920.3	Port 4	870	13.3	10.0	20	10	13.5
1	30	2.0	48.7	920.3	Port 8	810	13.3	10.0	20	10	13.5
2	39.5	1.5	64.0	906.1	Flame	1963[3]	16.2	10.0	20	10	16.4
2	39.5	1.5	64.0	906.1	Port 4	1090	13.2	10.0	20	10	13.5
2	39.5	1.5	64.0	906.1	Port 8	970	13.2	10.0	20	10	13.5
3	45	1.3	72.5	900.5	Port 4	1180	13.3	10.0	20	10	13.5

[1]Port temperatures were measured before atomization injector insertion, and do not include any localized temperature depression caused by the AFFF, atomizing air and the two injector sweep airs. These additional volumes add ~4% to the total combustion gas volumetric flow.
[2]Injector sweep air (1&2) are introduced co-centrically around the AFFF and atomizing air to minimize heating and thermal degradation of the AFFF within the atomizing injector.
[3]Calculated methane-air adiabatic flame temperature.

3.3.2 AFFF injection

One legacy AFFF formulation composed primarily of PFOS and perfluorohexanesulfonic acid (PFHxS) was used for these experiments. The AFFF was analyzed by a commercial laboratory for PFAS according to their liquid chromatography coupled to tandem mass spectrometry (LC/MS/MS) method derived from EPA Method 533.[26] The AFFF was added to a 19 L Cornelius keg placed on a scale to monitor mass loss and feed rate. The injection technique has been used previously[27] and is described here. AFFF was atomized through the burner or through one of two axial post-flame access ports along the furnace centerline using twin fluid (air/AFFF) atomizers, see Figure 5. The Cornelius keg was air pressurized (~584 kPa) to push the AFFF through a manually adjusted needle valve and 4-50 mL/min liquid rotameter (Brooks Instrument, Hatfield, PA) to the atomizer. The mass of the Cornelius keg was reported each minute to allow for the mass flow determination. Simultaneously, compressed air (584 kPa) was directed through a mass flow controller (Sierra Instruments, model Smart-Trak 50 L/min, Monterey, CA) to the atomizer. The AFFF and atomization air were combined at one end of a length of 0.1753 cm inside diameter, 0.3175 cm outside diameter stainless steel tubing. Within the tubing the atomizing air causes the liquid to form a thin film on the inner tube surface and shears the liquid film into droplets (~50 µm diameter for water) as it leaves the other end. The injector for the two post-flame axial access ports included a 90-degree bend at the atomizer tip to direct the atomized AFFF downstream co-current with the combustion gases along the furnace centerline. In addition, to mitigate the potential for pyrolysis, the side port atomizer included two additional concentric outer tubes through which additional "sweep" air was introduced to keep the AFFF and atomizing air cool until the atomizer tip. The volumes of these two cooling flows were minor (~3%) compared to the combustion gas flow. The burner incorporated atomizer did not need cooling, and atomized AFFF into the natural gas at the center of the International Flame Research Foundation (IFRF) variable air swirl burner (using setting 4 of 0-8) where the combined natural gas AFFF mixture then burned as a diffusion flame with combustion air added annularly.

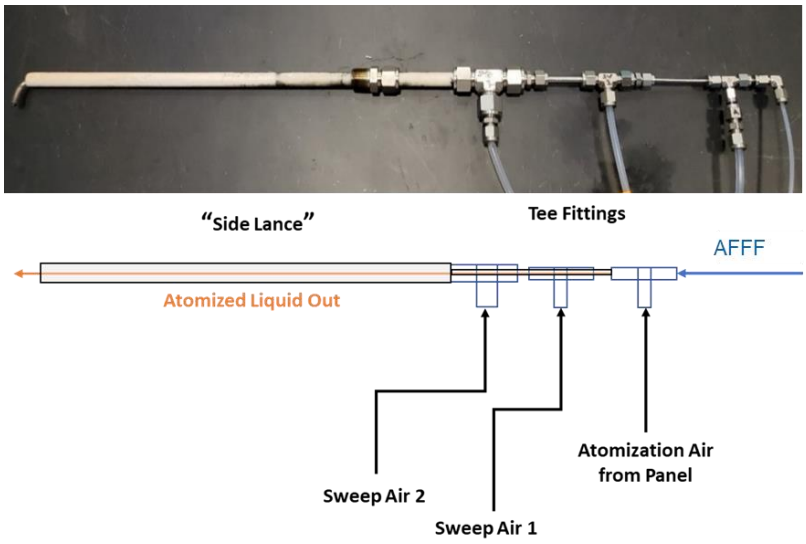

Figure 5. Twin fluid atomizer used to inject legact AFFF. AFFF was pushed through the small inner tube, atomized by Sweep Air 1, and cooled with Sweep Air 2.

3.3.3 Real-time measurements

Figure 4 indicates stack locations where combustion exhaust samples were extracted for analysis. As previously described,[22] a Fourier transform infrared spectrometer (FTIR, Model 2030, MKS Instruments Inc., Andover, MA) and a continuous emission monitor (CEM, Model ZRE Analyzer, California Analytical, Orange, CA) measured furnace exhaust concentrations of oxygen (O_2), carbon monoxide (CO), and CO_2. These measurements are intended to verify combustion conditions and quantify small amounts of air in-leakage caused by the facility's induced draft blower and operation at ~1.27 cm H_2O draft. FTIR was also used to measure moisture (H_2O), HF, sulfur dioxide (SO_2), and nitric oxide (NO). Note that CEM measurements are dry (moisture removed), and FTIR measurements are wet. The CEM and FTIR values were compared, taking into account the water, to verify the FTIR's measurements.

3.3.4 Volatile nonpolar fluorinated compounds

The nonpolar VFCs were sampled using a preliminary version of Other Test Method (OTM)-50.[13] Samples were taken using evacuated 6 L Silonite coated stainless steel canisters (Entech, Simi Valley, CA). The emissions were sampled with a heated probe, filter, and perfluoroalkoxy alkane (PFA) heated sample line at 120 °C and ~3 L/min. A 1.0 L/min slip stream of the emissions was passed through three 0.1 M sodium hydroxide (NaOH) filled mini (~30 mL) impingers and one empty impinger in an ice bath to remove acid gases and reduce the water content in the samples. The evacuated canisters (-101 kPa) collected stack gases after the impingers and were filled to ~-34 kPa, resulting in ~4 L sample volume. Sub-ambient pressure was maintained to minimize condensation inside the canister. For analysis, the canisters were spiked with internal standards, d5-chlorobenzene and 1,4-difluorobenzene, and pressurized with dry nitrogen to 207 kPa.

The canisters were analyzed using a Markes International Unity-xr TD system and Markes BenchTOF-Select MS system (Bridgend, UK) integrated with an Agilent 7890B gas chromatograph (GC, Santa Clara, CA). Tetrafluoromethane was concentrated from 15 mL of sample to avoid trap breakthrough. A 200 mL aliquot of the samples were trapped for other PFAS. Samples were concentrated using a Markes Greenhouse Gas trap at -30 °C and desorbed at 40 °C/s to 280 °C and held for 0.5 min. Analytes were separated using an Agilent GS-GasPro column (60 m x 0.32 mm inside diameter) starting at 50 °C, held for 1 min, increased at 5 °C/min to 130 °C and then ramped at 10 °C/min to 240 °C and held for 37 min. Quantitation of 30 vPFAS were performed using a seven-point (0.5 to 20 ppbv, 50 to 200 ppbv for CF4) calibration curve for each analyte.

3.3.5 Polar semi- and nonvolatile PFAS

The semivolatile and nonvolatile polar PFAS were sampled and analyzed according to the U.S. EPA's OTM-45.[12] Briefly, ~3.0 m^3 was sampled over three hours at a constant rate from the furnace exhaust. Due to the low pressure drop in the ductwork, isokinetic sampling could not be performed. OTM-45 creates four fractions (probe rinsate and filter, an XAD sorbent trap, impinger water, and a breakthrough XAD sorbent trap) for analysis using LC/MS/MS with a method based on Method 533 to quantify 49 polar PFAS, including PFOS, PFOA, and other common PFAS. The PFAS mass from each fraction was summed to give the total mass for each sample. A proof blank train was created by setting up and recovering an OTM-45 train with clean glassware near the sampling location. The sample extraction and analyses were performed by a commercial environmental laboratory, Eurofins TestAmerica (Knoxville, TN), according to OTM-45 and their standard operating procedures.

3.3.6 Calculation of destruction efficiency

To account for variable excess combustion air and any additional dilution caused by in leakage into the furnace, the DEs for the targeted PFAS in the AFFF were calculated using Method 19[28] as done previously.[22] The DE, or percent removal, was calculated using equation 1, but W_{out} was replaced with Method 19's E_{ao}, the mass emissions rate, and W_{in} was replaced with E_{ai}, the mass input rate.

$$DE\ or\ DRE = [1 - (E_{ao}/E_{ai})] \times 100\% \qquad (1)$$

3.4 PILOT SCALE FLUOROTELOMER BASED AFFF COMBUSTION

3.4.1 Furnace conditions and AFFF injection

The thermal treatment of an FT-based AFFF was carried out following most of the procedures in Section 3.3 and previous work.[29] The setup and modifications are explained here. The furnace conditions and AFFF injection rates are shown in Table 6. The natural gas and combustion air were varied to achieve peak AFFF injection temperatures from 760 to 1160 °C. The AFFF was injected at ports 4, 6, and 8, see Figure 4. A new water-cooled dual fluid injection lance, see Figure 6, was constructed to reduce the amount of air added to the furnace from the cooling sweep air used in Section 3.3, dropping to only 10 L/min from the 40 L/min used in 3.3.

Table 6. Rainbow furnace conditions for fluorotelomer based AFFF

Thermal load, kW	Stoich. ratio, SR	NG flow rate, L/min	Air flow rate, L/min	Injection location	Port temperature[1], °C	AFFF feed rate, g/min	AFFF feed rate, mL/min	Atomizing air flow rate, L/min
42	1.4	67.5	900	4	1160	13.5	13.0	10
42	1.4	67.5	900	6	1080	13.0	12.5	10
42	1.4	67.5	900	8	1010	14.7	14.1	10
34	1.72	55.5	910	8	880	13.0	12.5	10
28	2.1	46	920	4	860	13.4	12.9	10
28	2.1	46	920	8	760	13.4	12.9	10

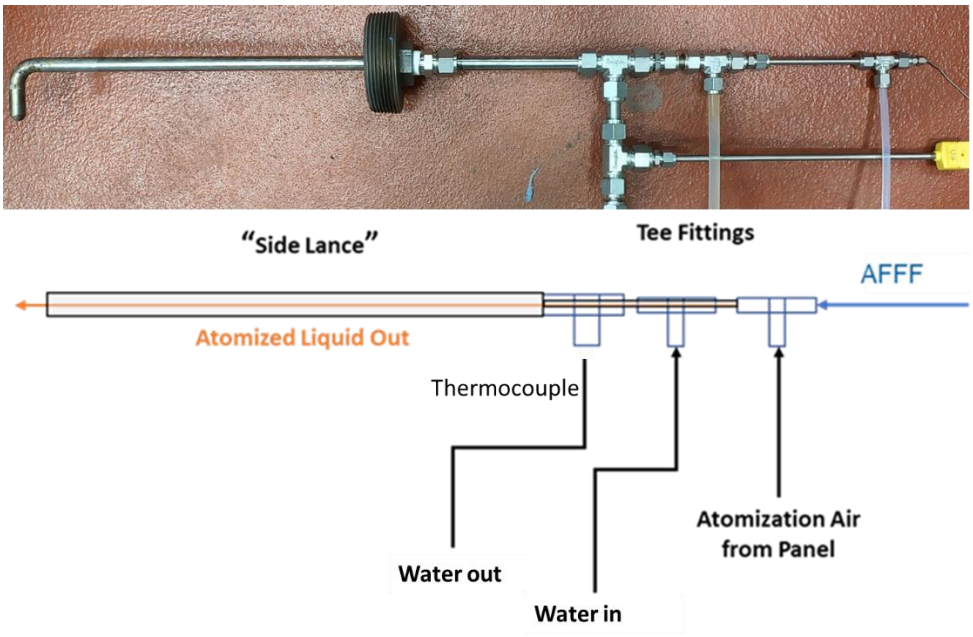

Figure 6. Water cooled injection lance

The AFFF was characterized by Pace Labs using their total oxidizable precursor assay (TOPA) to identify common PFAS and attempt to calculate the organic fluorine content of a 1000x dilution of the AFFF concentrate. Pace Labs also ran their adsorbable organic fluorine (AOF) method to determine how well the PFAS were oxidized during the TOPA. The specific gravity to determine the volume injections was found on the AFFF's safety data sheet.[30]

3.4.2 Hexafluoroethane injection

Co-injection of C_2F_6 with the AFFF was performed to evaluate the destruction of the PFC to attempt to correlate C_2F_6 destruction with the absence of PICs and destruction of PFAS. The C_2F_6 was added to the atomization air using a calibrated mass flow controller (Alicat Whisper 100SCCM, Tucson, AZ) set to inject 35.0 mL/min of C_2F_6, resulting in a concentration of 35 ppmv (201,000 $\mu g/m^3$).

3.4.3 Emissions sampling

The emissions from the incineration of the injections were mostly sampled as previously described in Section 3.3, any changes are briefly described here. The emissions were sampled prior to the APCS at the same locations listed in Section 3.3, Figure 4. Separate trains for OTM-45 and Method 0010 were sampled concurrently for 3 h for approximately a 3.8 m^3 sample. The OTM-45 train only had the breakthrough XAD trap for the lower temperature runs at 760 and 860 °C. The trains were recovered according to the methods, except the Method 0010 train was rinsed with acetone and methylene chloride that were collected separately.

The ports above the OTM-45 and Method 0010 were used for the FTIR probe and OTM-50 sampling. The FTIR was setup and used as described in Section 3.3 using a hybrid of Method 320 and ASTM D6348-12. OTM-50 used the train setup from the method that includes impingers to reduce the water and eliminate acid gases. The sample rate and volumes were controlled using critical orifices to collect a 4 – 5 L sample in about 2.5 h and about 24 minutes, #3 and #1 critical orifices, respectively, purchased from Entech Instruments (Simi Valley, CA).

3.4.4 Sample analyses

The OTM-45 samples were extracted and analyzed according to Eurofins' SOP. This used a different process to concentration the XAD extracts from the first edition of OTM-45. A 90 mL aliquot of the XAD extract was diluted in water to 1.0 L, and then extracted using an SPE cartridge. This provides similar detection limits to the original method but helps improve the extraction standard recoveries by better removing the excess water from the extract.

The Method 0010 train was extracted using Method 3542, a methylene chloride extraction of the fractions. The extracts were analyzed with GC/MS for fluorotelomer alcohols and Method 8270, semivolatile organics, with a library search to tentatively identify unknown peaks according to Eurofins' SOPs. The use of Method 0010 for sampling, Method 3542 for extraction, and an analytical method similar to Method 8270 is currently being developed into a yet to be released new OTM, OTM-55. OTM-55 will measure nonpolar semivolatile fluorinated compound in emissions.

The OTM-50 canister samples were analyzed with GC/MS according to OTM-50 and the Jacobs Engineering SOP. The method has changed little from Section 3.3. The following describes some of the changes from above to make the SOP match up better to OTM-50. The calibrations were performed using individual canisters for each concentration and the normal method injection volume. The acceptance criteria for the standards to match the calibrated values was tightened to ±20% from 30% used previously.

4.0 RESULTS AND DISCUSSION

4.1 BENCH SCALE PERFLUOROCARBON THERMAL DESTRUCTION

In the bench scale study, the destruction efficiency (DE), mineralization efficiency (ME), and F mass balance are defined as follows:

Destruction Efficiency

How much parent FC was altered or destroyed, not necessarily complete mineralization to HF.

$$DE\ (\%) = \left(1 - \frac{FC\ Recovered}{FC\ Introduced}\right) x\ 100 \qquad \text{----- (2)}$$

Mineralization Efficiency

How much FC was completely mineralized to HF and CO_2. This was calculated based on the F added to the system (F introduced as FC) and the inorganic F measured at the outlet (F recovered as HF). Formation of SiF_4 was often observed, which is believed to be a result of the HF reaction with the quartz reactor wall. Therefore, if SiF_4 was observed, it was accounted as HF. One mole of SiF_4 is considered to be equivalent to four moles of HF.

$$ME\ (\%) = \left(\frac{F\ Recovered\ as\ HF}{F\ Introduced\ as\ FC}\right) x\ 100 \qquad \text{----- (3)}$$

F Mass Balance

How much F was recovered in any form at the reactor exit (F recovered in any form) relative to the F introduced as the FC.

$$F\ Mass\ Balance\ (\%) = \left(\frac{F\ Recovered\ in\ Any\ Form}{F\ Introduced\ as\ FC}\right) x\ 100 \qquad \text{----- (4)}$$

Tables 7, 9, 11, 13, and 15 show the thermal treatment profiles of CF_4, C_2F_6, C_3F_8, C_4F_{10}, and C_5F_{12} in air, respectively. Tables 8, 10, 12, 14, and 16 show the thermal treatment profiles of CF_4, C_2F_6, C_3F_8, C_4F_{10}, and C_5F_{12} in N_2, respectively. The 3rd row, Bypass, is the initial parent compound concentrations measured without thermal treatment, the FC introduced. The gases were bypassed the reactor and directly measured by FTIR. This value was used to calculate total F, DE, ME, and F mass balance. The compounds name below "Bypass" and above "Total F" are the concentrations of PIDs and HF detected by FTIR in ppm. Total F is the total amount of F calculated based on the remaining FC, PID, and HF concentrations in ppm (F recovered in any form). The Expected F is the F introduced as FC, the calculated F concentration based on the parent compound's bypass concentration and the number of F the parent compound contains in ppm. The DE, ME, and F Mass Balance were calculated based on the equations (1) to (3) shown above.

Tables 7 and 8 show the thermal treatment profiles of CF_4 in the air and N_2 environments, respectively. The destruction and mineralization profiles in both environments were similar, but a greater DE and ME were observed in the N_2 environment at 1400 °C. Over 99% DE was observed at 1600 °C in both environments. The carbonyl fluoride (CF_2O) was the only PID observed. The DE and ME increased as temperature and residence time increased in general; however, the ME

decreased when the residence time increased from 2 to 4 s at 1450 °C and from 1 to 2 s at 1600 °C. It is speculated that either CF_4 directly reacted with the alumina reactor or formed HF reacted with the alumina reactor, chemically formed aluminum – fluorine bond, and deposited on the wall. As a result, F did not come out as gas species and resulted in lower ME. A lower F mass balance with longer residence time supports the above hypothesis. The surface analysis of the reactor wall, such as X-ray photoelectron spectroscopy (XPS), may elucidate it. A slight DE and ME were observed at 1300 °C, and a complete decomposition was observed at 1600 °C.

Table 7. CF_4 Thermal Treatment Profile in Air

Temp. (°C)	1300	1450			1600	
Res. Time (s)	4	1	2	4	1	2
Bypass (ppm)	101.8	102.3	100.5	101.8	102.3	100.5
CF_4 (ppm)	96.5	93.6	59.8	38.4	0.8	0.2
HF (ppm)	10.8	64.3	97.4	28.0	258.2	207.2
CF_2O (ppm)	<0.1	<0.1	0.2	0.4	2.4	5.0
Total F (ppm)	396.7	438.6	337.0	182.5	266.3	217.7
Expected F (ppm)	407.2	409.2	402.0	407.2	409.2	402.0
DE (%)	5.2	8.6	40.5	62.3	99.2	99.9
ME (%)	5.8	16.6	27.3	17.3	67.0	61.1
F Mass Balance (%)	97.4	107.2	83.8	44.8	65.1	54.2

Table 8. CF_4 Thermal Treatment Profile in N_2

Temp. (°C)	1300	1450			1600	
Res. Time (s)	4	1	2	4	1	2
Bypass (ppm)	105.6	110.2	101.7	105.6	110.2	101.7
CF_4 (ppm)	95.2	74.2	37.2	12.5	0.2	0.1
HF (ppm)	9.6	133.3	158.6	39.9	296.1	230.2
CF_2O (ppm)	<0.1	<0.1	<0.1	<0.1	<0.1	0.1
Total F (ppm)	390.4	429.9	307.4	89.8	296.9	230.9
Expected F (ppm)	422.4	440.8	406.8	422.4	440.8	406.8
DE (%)	9.8	32.7	63.4	88.2	99.8	99.9
ME (%)	4.2	31.6	44.6	23.3	70.3	65.3
F Mass Balance (%)	92.4	97.5	75.6	21.3	67.4	56.8

Tables 9 and 10 show the thermal treatment profiles of C_2F_6 in the air and N_2 environments, respectively. The decomposition and destruction profiles in both environments were similar. Complete destruction was observed at 1000 °C 4 s and 1150 °C 2 s in both environments. A large amount of CF_2O was observed as a PID in both environments, with the concentration increasing when the temperature increased to 1000 °C but then decreasing when the temperature increased to 1150 °C. The investigation of the longer residence time at 1150 °C is desirable to elucidate the fate of CF_2O. Other PIDs observed were a small amount of SiF_4, which was formed by the gas-surface reactions between fluorinated compounds and fused silica quartz reactor wall. A small amount of CF_3H was also observed at 850 °C in the N_2 environment. Both the destruction and mineralization increased as temperature and residence time increased, but the mineralization did not improve by more than 50 – 60 %. A lower F mass balance was observed as the temperature

and the residence time increased. Both phenomena are believed to be due to the lower HF transport efficiency as temperature and residence time increased.

Table 9. C_2F_6 Thermal Treatment Profile in Air

Temp. (°C)	**850**		**1000**		**1150**
Res. Time (s)	2	4	2	4	2
Bypass (ppm)	119.6	121.8	119.6	121.8	119.6
C_2F_6 (ppm)	118.1	114.6	9.06	0.1	<0.1
HF (ppm)	8.7	26.1	285.2	377.2	387.9
CF_2O (ppm)	4.4	13.3	164.1	83.1	55.1
SiF_4 (ppm)	<0.1	0.1	<0.1	3.3	<0.1
CF_3H (ppm)	<0.1	<0.1	<0.1	<0.1	<0.1
Total F (ppm)	726.1	740.7	667.8	557.2	498.1
Expected F (ppm)	717.6	730.8	717.6	730.8	717.6
DE (%)	1.3	5.9	92.4	99.9	>99.9
ME (%)	1.2	3.6	39.7	53.4	54.1
F Mass Balance (%)	101.2	101.4	93.1	76.2	69.4

Table 10. C_2F_6 Thermal Treatment Profile in N_2

Temp. (°C)	**850**		**1000**		**1150**
Res. Time (s)	2	4	2	4	2
Bypass (ppm)	111.9	113.2	111.9	113.2	111.9
C_2F_6 (ppm)	115.7	110.8	3.8	0.0	0.0
HF (ppm)	6.5	22.5	263.9	274.8	286.3
CF_2O (ppm)	4.7	12.3	150.8	81.5	77.1
SiF_4 (ppm)	<0.1	0.1	0.4	1.6	0.6
CF_3H (ppm)	2.5	5.4	<0.1	<0.1	<0.1
Total F (ppm)	717.8	728.5	589.6	444.4	442.8
Expected F (ppm)	671.4	679.2	671.4	679.2	671.4
DE (%)	1.0	2.1	96.6	>99.9	>99.9
ME (%)	1.0	3.4	39.5	41.4	43.0
F Mass Balance (%)	106.9	107.3	87.8	65.4	66.0

Tables 11 and 12 show the thermal treatment profiles of C_3F_8 in the air and N_2 environments, respectively. The destruction and mineralization profiles in both environments were similar. Destruction was observed at 850 °C and 8 s and the higher temperatures in both environments. The profile of the PID was different in the air and N_2 environments. The concentration of CF_2O was higher in the air environment than in the N_2 environment. The concentration of CF_2O increased when the temperature increased to 1000 °C but then decreased when the temperature increased to 1150 °C. The investigation of the longer residence time at 1150 °C is desirable to elucidate the fate of CF_2O. Other PIDs observed were SiF_4, CF_3H, and C_2F_6. The formation of CF_3H and C_2F_6 was mainly observed in the N_2 environment at 850 °C and disappeared at the higher temperature. The ME increased as the temperature and residence time increased but did not improve by more than 50 – 60%. A lower F mass balance was observed as the temperature

and the residence time increased. Same as the C_2F_6 case, these are believed to be due to the lower HF transport efficiency as temperature and residence time increased.

Table 11. C_3F_8 Thermal Treatment Profile in Air

Temp. (°C)	850			1000			1150	
Res. Time (s)	2	4	8	2	4	8	2	4
Bypass (ppm)	111.5	118.1	111.5	111.5	118.1	111.5	111.5	118.1
C_3F_8 (ppm)	51.0	0.0	0.0	0.0	0.0	0.0	0.0	0.0
HF (ppm)	149.7	383.7	317.8	336.8	428.9	284.8	440.6	467.0
CF_2O (ppm)	162.3	304.4	165.1	305.3	114.6	21.3	93.7	11.6
SiF_4 (ppm)	0.3	4.2	17.9	0.5	6.8	34.7	1.0	7.7
CF_3H (ppm)	17	1.5	<0.1	<0.1	<0.1	<0.1	<0.1	<0.1
C_2F_6 (ppm)	<0.1	<0.1	<0.1	<0.1	<0.1	<0.1	<0.1	<0.1
Total F (ppm)	934.5	1013.8	719.4	949.4	685.2	466.3	631.8	521.1
Expected F (ppm)	892.0	944.8	892.0	892.0	944.8	892.0	892.0	944.8
DE (%)	54.3	>99.9	>99.9	>99.9	>99.9	>99.9	>99.9	>99.9
ME (%)	16.9	42.4	43.6	38.0	48.3	47.5	49.8	52.7
F Mass Balance (%)	104.8	107.3	80.7	106.4	72.5	52.3	70.8	55.1

Table 12. C_3F_8 Thermal Treatment Profile in N_2

Temp. (°C)	850			1000			1150	
Res. Time (s)	2	4	8	2	4	8	2	4
Bypass (ppm)	110	116	110	110	116	110	110	116
C_3F_8 (ppm)	71.0	22.0	<0.1	<0.1	<0.1	<0.1	<0.1	<0.1
HF (ppm)	91.2	220.9	252.1	397.6	445.4	405.0	463.9	493.7
CF_2O (ppm)	63.8	107.2	65.9	239.7	154.3	49.9	114.9	27.0
SiF_4 (ppm)	<0.1	0.8	11.7	0.7	3.3	31.6	1.2	4.3
CF_3H (ppm)	47	41	16.5	1.7	<0.1	<0.1	<0.1	<0.1
C_2F_6 (ppm)	10	13	9.6	5.0	<0.1	<0.1	<0.1	<0.1
Total F (ppm)	987.8	815.7	538.0	914.8	767.3	631.0	698.4	564.8
Expected F (ppm)	880.0	928.0	880.0	880.0	928.0	880.0	880.0	928.0
DE (%)	35.5	81.0	>99.9	>99.9	>99.9	>99.9	>99.9	>99.9
ME (%)	10.4	24.2	34.0	45.5	49.4	60.4	53.2	55.0
F Mass Balance (%)	112.2	87.9	61.1	104.0	82.7	71.7	79.4	60.9

Tables 13 and 14 show the thermal treatment profiles of C_4F_{10} in the air and N_2 environments, respectively. C_4F_{10} was destroyed at all experimental conditions, starting at 850 °C and 2 s. The profile of the PIDs was different in the air and N_2 environments. The concentration of CF_2O was much higher in the air environment than in the N_2 environment. A CF_3H was observed mostly in the N_2 environment, and it decreased as the temperature and residence time increased. Low concentrations of C_2F_6 were observed in both environments. The ME increased as the temperature and residence time increased but did not improve by more than 40 – 50%. A lower F mass balance was observed as the temperature and the residence time increased. These are believed to be due to the lower HF transport efficiency as temperature and residence time increased.

Table 13. C_4F_{10} Thermal Treatment Profile in Air

Temp. (°C)	850		1000		1150	
Res. Time (s)	2	4	2	4	2	4
Bypass (ppm)	115.0	118.0	115.0	118.0	115.0	118.0
C_4F_{10} (ppm)	<0.1	<0.1	<0.1	<0.1	<0.1	<0.1
HF (ppm)	292.3	424.7	376.4	454.6	478.0	504.3
CF_2O (ppm)	476.7	311.4	404.5	243.7	125.3	12.4
SiF_4 (ppm)	0.5	4.3	1.1	6.8	3.7	9.0
CF_3H (ppm)	<0.1	<0.1	<0.1	<0.1	<0.1	<0.1
C_2F_6 (ppm)	<0.1	<0.1	<0.1	<0.1	<0.1	<0.1
Total F (ppm)	1247.5	1064.5	1189.9	969.1	743.3	564.9
Expected F (ppm)	1150.0	1180.0	1150.0	1180.0	1150.0	1180.0
DE (%)	>99.9	>99.9	>99.9	>99.9	>99.9	>99.9
ME (%)	25.6	37.4	33.1	40.8	42.8	45.8
F Mass Balance (%)	108.5	90.2	103.5	82.1	64.6	47.9

Table 14. C_4F_{10} Thermal Treatment Profile in N_2

Temp. (°C)	850		1000		1150	
Res. Time (s)	2	4	2	4	2	4
Bypass (ppm)	114.9	118	114.9	118	114.9	118
C_4F_{10} (ppm)	<0.1	<0.1	<0.1	<0.1	<0.1	<0.1
HF (ppm)	241.7	359.1	452.4	493.4	438.6	386.2
CF_2O (ppm)	155.3	186.6	261.2	167.7	77.6	7.7
SiF_4 (ppm)	0.3	2.8	0.9	5.0	0.9	1.9
CF_3H (ppm)	63.7	36.3	2.2	5.9	0.4	<0.1
C_2F_6 (ppm)	<0.1	<0.1	<0.1	<0.1	<0.1	<0.1
Total F (ppm)	1073.4	1126.9	1006.2	866.4	598.4	409.3
Expected F (ppm)	1149.0	1180.0	1149.0	1180.0	1149.0	1180.0
DE (%)	>99.9	>99.9	>99.9	>99.9	>99.9	>99.9
ME (%)	21.2	31.4	39.7	43.5	38.5	33.4
F Mass Balance (%)	93.4	95.5	87.6	73.4	52.1	34.7

Tables 15 and 16 show the thermal treatment profiles of C_5F_{12} in the air and N_2 environments, respectively. Like C_4F_{10}, C_5F_{12} was destroyed at all experimental conditions, starting at 850 °C and 2 s. The profile of the PID was different in the air and N_2 environments. The concentration of CF_2O was much higher in the air environment than in the N_2 environment at 850 °C, and it decreased with the temperature and residence time increased. The concentration of CF_3H was much higher in the N_2 environment at 850 °C, and it decreased as temperature and residence time increased. No C_2F_6 was observed. The ME increased as the temperature and residence time increased but did not improve by more than 40 – 50%. A lower F mass balance was observed again as the temperature and the residence time increased. These are believed to be due to the lower HF transport efficiency as temperature and residence time increased.

Table 15. C_5F_{12} Thermal Treatment Profile in Air

Temp. (°C)	850			1000			1150		
Res. Time (s)	2	4	8	2	4	8	2	4	8
Bypass (ppm)	123.1	115.5	115.4	123.1	115.5	115.4	123.1	115.5	115.4
C_5F_{12} (ppm)	<0.1	<0.1	<0.1	<0.1	<0.1	<0.1	<0.1	<0.1	<0.1
HF (ppm)	404.0	435.9	420.0	455.0	497.6	480.7	504.3	538.7	522.6
CF_2O (ppm)	524.5	480.0	374.0	439.0	295.1	148.5	186.7	30.6	0.6
SiF_4 (ppm)	0.9	3.0	20.2	5.7	3.6	27.5	1.7	4.6	31.3
CF_3H (ppm)	5.6	4.9	3.7	4.3	2.8	1.5	1.9	0.3	<0.1
C_2F_6 (ppm)	<0.1	<0.1	<0.1	<0.1	<0.1	<0.1	<0.1	<0.1	<0.1
Total F (ppm)	1488.3	1429.8	1268.9	1368.8	1110.7	892.2	890.0	619.3	648.8
Expected F (ppm)	1477.2	1386.0	1384.8	1477.2	1386.0	1384.8	1477.2	1386.0	1384.8
DE (%)	>99.9	>99.9	>99.9	>99.9	>99.9	>99.9	>99.9	>99.9	>99.9
ME (%)	27.6	32.3	36.2	32.3	36.9	42.7	34.6	40.2	46.8
F Mass Balance (%)	100.8	103.2	91.6	92.7	80.1	64.4	60.3	44.7	46.9

Table 16. C_5F_{12} Thermal Treatment Profile in N_2

Temp. (°C)	850			1000			1150		
Res. Time (s)	2	4	8	2	4	8	2	4	8
Bypass (ppm)	121.1	120.7	111.8	121.1	120.7	111.8	121.1	120.7	111.8
C_5F_{12} (ppm)	0.0	0.0	0.0	0.0	0.0	0.0	0.0	0.0	0.0
HF (ppm)	270.1	405.6	410.4	480.0	515.9	490.2	524.4	539.8	529.7
CF_2O (ppm)	128.8	172.8	139.2	333.5	293.1	143.8	167.1	50.4	2.6
SiF_4 (ppm)	0.5	1.9	15.1	1.3	4.4	21.0	1.9	4.8	32.1
CF_3H (ppm)	57.5	42.2	18.2	5.0	2.9	1.5	1.7	0.6	<0.1
C_2F_6 (ppm)	<0.1	<0.1	<0.1	<0.1	<0.1	<0.1	<0.1	<0.1	<0.1
Total F (ppm)	1199.4	1360.2	1172.7	1205.1	1128.1	866.3	871.2	661.7	663.3
Expected F (ppm)	1453.2	1448.4	1341.6	1453.2	1448.4	1341.6	1453.2	1448.4	1341.6
DE (%)	>99.9	>99.9	>99.9	>99.9	>99.9	>99.9	>99.9	>99.9	>99.9
ME (%)	18.7	28.5	35.1	33.4	36.8	42.8	36.6	38.6	49.1
F Mass Balance (%)	82.5	93.9	87.4	82.9	77.9	64.6	59.9	45.7	49.4

4.2 PILOT SCALE FLUOROCARBON THERMAL DESTRUCTION

As described by Tsang et al.,[11] CF_4 is the most difficult fluorocarbon to dissociate, as its strong symetrical C-F bonds (552 kJ/mol) are extremely difficult to break through unimolecular decomposition. In contrast, the relatively weak HO-F bond (216 kJ/mol) formed through reaction with a hydroxide radical (OH) makes this pathway non-viable. This leaves the attack of the C-F bonds by H radicals to form more stable H-F bonds (569 kJ/mol) as the only viable CF_4 dissociation pathway. However, H radicals are not expected to persist in high concentrations far outside fuel-rich flame regions, as they tend to readily form OH in the strongly oxidative post-flame region. C_2F_6 has a relatively weak C-C bond (408 kJ/mol) which is lower than the C-H bond for CHF_3 (456 kJ/mol). For C_2F_6, unimolecular C-C dissociation seems to be the preferred pathway, and the relatively higher energy required to break the C-C bond will make subsequent decomposition of the weaker CF_2-F bond (352 kJ/mol) viable. However, the resulting symmetrical CF_2 radicals formed subsequently have relatively strong C-F bond energies (508 kJ/mol), and

further decomposition of the CF_2 radicals will be more difficult with significant potential for PIC formation.

Table 17 presents DE calculations based on FTIR measurements for CF_4, CHF_3, and C_2F_6 introduced with the natural gas (through the flame), combustion air, and at selected post-flame locations. Results for 40, 45, and 64 kW furnace loads are included. DEs. Calculation of DEs for both the measurements and model were based on EPA Method 19 (U.S. EPA, 2017) and include volume corrections based on the natural gas fuel composition (stoichiometry) and use measured CO_2 (wet) concentrations to adjust for small amounts of in leakage caused by the combustor's induced draft blower. Evident from Table 17 is that DEs for CF_4 are less than 60, 90, and 95% for 40, 45, and 64 kW loads, respectively, even when introduced through the flame. Introduced further downstream at post-flame conditions, CF_4 DEs are very consistent, decreasing from ~14% (45 kW, Port 4, 1295 °C) to ~8% (40 kW, Port 11, ~875 °C). Clearly, even directly exposed to flames, CF_4 is very difficult to destroy, and we postulate that the nearly constant (perhaps slowly declining) DEs of CF_4 downstream of the flame may be related to partial catalytic destruction of CF_4 on the alumina-rich high temperature refractory lining the Rainbow furnace or interference due to water with the FTIR. CF_4 is used for plasma etching purposes in several industries including semiconductor production, and metal catalysts, including γ-alumina, are used as a control technology to catalytically oxidize residual CF_4.[31] Calculation of the relative time scales for diffusion and advection suggests that while mass transfer by advection dominates, there is sufficient residence time for a portion of the CF_4 to diffuse to and react with the refractory walls. At 45 and 64 kW, we compared measured DEs for CF_4 introduced with the natural gas and combustion air. Both are introduced through the burner, but each experience a different oxidizing/reducing environment and temperature history. Interestingly, DEs for CF_4 introduced with the natural gas 90 and 95% are higher than for CF_4 introduced with the combustion air 83 and 89% (45 and 64 kW, see Table 17). The increased DE through natural gas in the burner suggests mixing CF_4 with hydrogen at the diffusion flame front may be beneficial for the destruction of C-F bonds through free radical reaction mechanisms. Our observations indicate premixing natural gas with CF_4 to make more hydrogen radicals readily available in the flame facilitates destruction of C-F bonds.

In contrast to CF_4, measured DEs for CHF_3 are very high (>99.9%). Even at 40 kW when introduced at Port 12 (830 °C), the DE is ~94%. Model calculations and species profiles predict significant concentrations of OH radicals persist for seconds post-flame through Ports 10 and 12 (0.035 and 0.017 ppmv, respectively), so hydrogen abstraction by OH accounts for the high DEs determined for CHF_3 when introduced at these relatively moderate temperature locations. However, as indicated in Figure 7, high DE does not necessarily mean the absence of PICs, as hydrogen abstraction of the CF_3-H bond results in the formation of trifluoromethyl (CF_3) radicals which can undergo further reactions including reactions with other fluorinated species. Figure 6 (45 kW) shows example FTIR traces during experiments where CHF_3 was injected at Port 10 (1060 °C) and Port 12 (984 °C) locations, well downstream of the flame. Real-time measurements were acquired not only for the CHF_3 that was being injected, but also for the CF_4 and C_2F_6 that were formed as PICs. Figure 7 also presents HF, as well as the CO_2 and H_2O generated predominantly in the flame. Concentrations of multiple species spanning six orders of magnitude were measured simultaneously. Evident from Figure 7 is that even though CHF_3 concentrations are below detection levels when introduced at 1060 and 984 °C, ports 10 and 12

respectively, and DEs >99% are achieved, CF_4 emissions (~0.10 ppmv) are evident at 1060 °C, and CF_4 and C_2F_6 emissions (~0.08 and ~0.30 ppmv, respectively) are evident for 984 °C.

The thermal stability of C_2F_6 lies somewhere in between CF_4 and CHF_3. The measured DEs for C_2F_6 are >99% inside the flame zone and through Port 10 (1060 °C) but drop to ~86% at 984 °C. At 40 kW, DEs fell to ~78% at Port 8 (960 °C) and decreased rapidly from there. It appears that destruction of this simple perfluoro compound occurs near the flame zone where high temperature unimolecular dissociation and free radical reactions, likely involving H radicals, are the predominant destruction mechanisms. We believe that C_2F_6 may be an important potential surrogate PFAS compound for combustion studies because its single C-C bond is analogous to the multiple C-C bonds in larger PFAS. While CHF_3 may model the behavior of polyfluoro species compared to perfluoro species, C_2F_6 models C-C dissociation reactions common to almost all PFAS.

Table 17. Fluorocarbon destruction efficiencies

Temperature (°C)	DE (%)		
	CF_4	CHF_3	C_2F_6
Combustion air	88.7	>99	>99
Natural gas	94.9	>99	>99
1295	13.7	>99	>99
1203	12.9	>99	>99
1127	11.7	>99	>99
1090	-	>99	>99
1060	12.5	>99	>99
984	-	>99	86.2
960	-	-	78.2
930	-	>99	25.5
830	-	94.3	0

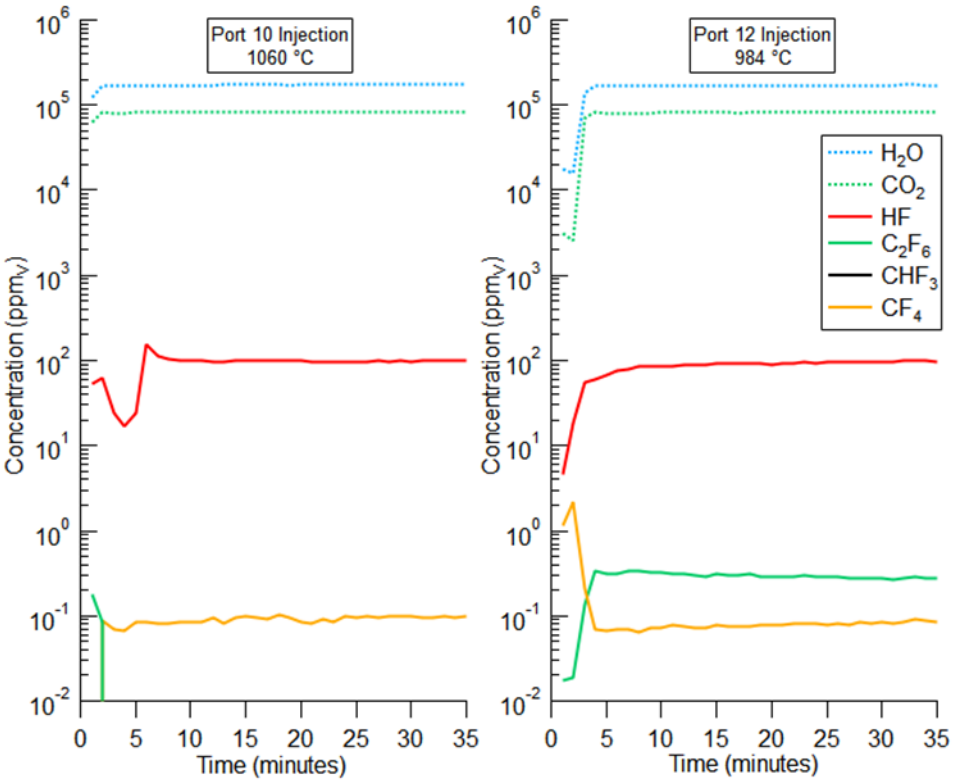

Figure 7. Real-time FTIR species concentrations depicting CHF_3 injection at ports 10 and 12 in the pilot-scale furnace

4.3 PILOT SCALE LEGACY AFFF COMBUSTION

4.3.1 Targeted PFAS destruction

The AFFF was found to contain 10 PFAS from the targeted analyte list, see Table 18. The quantitated PFAS consisted of C4 to C8 perfluoroalkyl carboxylic acids (PFCAs) and perfluoroalkyl sulfonic acids (PFSAs), and concentrations of the 10 PFAS were used to calculate the DEs for the PFAS in the AFFF. The PFAS found in the stack emissions from the OTM-45 sampling for all six AFFF injections are shown in Table 19, with compound abbreviations defined in Table 18. No other PFAS from the OTM-45 target list above method blank (MB) and reporting levels were detected in any of the sampling trains besides the original 10, with just perfluorononanoic acid (PFNA) being detected near blank levels in two samples and perfluorooctanesulfonamide (FOSA) being just above the detection limit in one sample. This is not surprising, as the 49 PFAS from OTM-45 are from methods for water analysis and are complex polar structures of industrial relevance that are more likely to be found in industrial discharges than to be formed via de novo synthesis during combustion processes. An exception to this may be the PFCAs which may form from fluoroalkyl fragments in the presence of water at post-flame and stack conditions.

Table 18. Legacy AFFF targeted PFAS content

Compound	ppb (ng/g)	weight %
Perfluorobutanoic acid (PFBA)	6850	0.000685
Perfluorobutanesulfonic acid (PFBS)	202000	0.0202
Perfluoropentanoic acid (PFPeA)	34100	0.00341
Perfluoropentanesulfonic acid (PFPeS)	164000	0.0164
Perfluorohexanoic acid (PFHxA)	111000	0.0111
Perfluorohexanesulfonic acid (PFHxS)	1180000	0.118
Perfluoroheptanoic acid (PFHpA)	31600	0.00316
Perfluoroheptanesulfonic acid (PFHpS)	136000	0.0136
Perfluorooctanoic acid (PFOA)	123000	0.0123
Perfluorooctanesulfonic acid (PFOS)	8020000	0.802
Targeted Organic Fluorine	6410000	-

Table 19. OTM-45 results for the legacy AFFF tests (ng/sample)

Temperature (°C)	MB[a]	PTB[a]	Flame	1180*	1090	970	870	810
Sample volume (dscm)[b]	-	-	3.12	3.71	3.71	3.72	3.74	3.74
Injection Port	-	-	-	4	4	8	4	8
PFAS (ng/sample)								
PFBA	ND	5.57	22.3	108	9.10[c]	628[c]	3950	116000
PFPeA	ND	3.32	17.6	56.0	7.42[c]	249[c]	741	63400
PFHxA	ND	6.59	26.1	100	13.8	490	1240	151000
PFHpA	0.40	1.55	6.32	29.8	5.23	65.5	475	36300
PFOA	ND	2.30	36.8	156	144[d]	452[d]	1434	78400
PFBS	0.11	0.41	0.61	6.66	0.57	0.67	28.8	1860
PFPeS	ND	ND	ND	4.58	0.14	0.54	23.4	1680
PFHxS	ND	1.25	0.92	21.6	1.36[d]	2.33[d]	118	8520
PFHpS	ND	ND	ND	1.84	ND	0.34	17.1	989
PFOS	ND	9.30[d]	3.08[d]	116	42.2[d]	18.6[d]	819	62200

a. MB is the analytical method blank and PBT is the proof blank train.
b. Sample volume is in dry standard cubic meters.
c. Pre-extraction internal standard over acceptance criteria
d. Pre-extraction internal standard under acceptance criteria
* 1180 °C run may have contamination by carryover from the 810 °C run

For these experiments, the train's glassware was cleaned according to OTM-45 for each test, so a field blank train was not run since the proof blank train (PBT) was the same as a field blank train. The PBT showed some near detection limit levels of contamination, mainly due to the XAD fractions of the train. The PFCAs, perfluorobutanesulfonic acid (PFBS), perfluorohexanesulfonic acid (PFHxS), and PFOS were all measured at trace levels in the proof blank train. The results are reported according to OTM-45, without any blank correction. The

samples with low levels of PFAS are reported as near blank levels to indicate that the result may be biased high and the PFAS may be below the detection limit. The OTM-45 data were also impacted by the low recovery of the isotopically labeled extraction internal standard for some longer chain PFAS. This is likely due to the water that collects in the XAD decreasing the solubility of the long chain PFAS. The impacted PFAS are noted in the tables, and the values are the highest estimated value provided by the commercial laboratory.

The experimental sequence was flame, 1090, 970, 870, 810, and 1180 °C. It appears that there may have been some hysteresis due to contamination of internal furnace surfaces after the test at the lowest temperature. Experiments were performed on separate days with at least 18 hours of operation at new combustion conditions without AFFF injection to achieve equilibrium. The experiment at 1180 °C was performed the day after the lowest temperature injection experiment at 810 °C and Table 19 indicates slightly higher concentrations of some PFCAs than the experiment at 1090 °C, and the PFSAs had higher concentrations than the experiment at 970 °C. Even so, the concentrations were not far above the detection limits and still show very high DEs, but the potential for hysteresis is something to note. The apparent carryover could be due to the quartz probe not going through an extensive cleaning process and only being rinsed and brushed, or the furnace may not have fully desorbed PFAS deposited on refractory and ductwork surfaces during the previous 810 °C experiment. Future tests will involve a combustion blank to look for contamination in the system and more time will pass between low temperature tests to allow more complete surface desorption.

The DEs for the 10 PFAS quantified in the AFFF as determined using Method 19 are shown in Table 20. The original PFAS concentrations (Table 18), AFFF feed rates and combustion parameters (Table 5), and AFFF stack emissions (Table 19) were used in the calculations. When reported PFAS emissions were not detected (ND), the detection limit was used as a conservative value for DE calculation. The lack of corrections for blank contamination as well as corrections for recoveries (including low recoveries) also serve to reduce DE values and provide more conservative values.

The DEs for all five PFSAs are >99.9999% for the four PFAS injection locations >970 °C. Even at 870 and 810 °C, DEs for all five PFSAs were >99.999% and >99.9%, respectively. DEs for the five PFCAs were also high (mostly >99.99%) for injection temperatures >1090 °C, and mostly >99.9% for injection temperatures >870 °C. Even at the lowest AFFF injection temperature, 810 °C, DEs >94% were measured for four PFCAs, except for perfluorobutanoic acid (PFBA). PFBA exhibited the lowest DEs, both with respect to AFFF injection temperatures and PFCA chain length. Lower than expected DEs for PFBA and PFCAs have been reported previously with various destruction technologies[32-34] and may suggest either that shorter PFCAs are relatively more stable species or shorter chained PFCAs are formed via hydrolysis of fluoroalkyl fragments in the post-flame. Note that PFSAs do not indicate this same trend with calculated DEs for PFBS and PFOS approximately similar at corresponding temperatures. This trend for PFCAs might also suggest a pathway or intermediate through which PFAS transition during thermal destruction. PFAS might be affected by high concentrations of hydroxyl radicals (OH), H_2O, and CO_2 in the combustion gases that promote reformation of PFCAs from fluoroalkyl fragments. This has been reported to occur in the atmosphere[35] and experimentally[36, 37], and the formation of aldehydes and acyl fluorides that can react to create carboxylic acids has been predicted by several computational mechanisms[38-41]. If true, this could reduce apparent DEs for PFCAs and explain the higher DEs for PFSAs. These experiments, using a complex mixture of PFAS and other unknown components in the AFFF, do not represent the best approach for addressing mechanistic questions. Further

experiments using neat solutions of specific PFAS in coordination with ongoing kinetic modeling efforts are needed to better address mechanisms.

Table 20. Destruction efficiencies for targeted PFAS

Temperature (°C)	Flame	1180	1090	970	870	810
PFAS	(%)	(%)	(%)	(%)	(%)	(%)
PFBA	99.9958	99.9725	99.9978	99.8443[b]	98.3336[b]	45.7362
PFPeA	99.9993	99.9971	99.9996	99.9876[b]	99.9372[b]	94.0300
PFHxA	99.9997	99.9984	99.9998	99.9925	99.9678	95.6188
PFHpA[a]	99.9997	99.9984	99.9997	99.9965	99.9566	96.3086
PFOA	99.9996	99.9978	99.9981	99.9938[b]	99.9663	97.9522
PFBS[a]	>99.9999	>99.9999	>99.9999	>99.9999	99.9996	99.9704
PFPeS	>99.9999	>99.9999	>99.9999	>99.9999	99.9996	99.9671
PFHxS	>99.9999	>99.9999	>99.9999[b]	>99.9999[b]	99.9997	99.9768
PFHpS	>99.9999	>99.9999	>99.9999	>99.9999	99.9996	99.9766
PFOS	>99.9999[b]	>99.9999	>99.9999[b]	>99.9999	99.9997	99.9751

[a] PFBS and PFHpA were detected in the analytical method blanks.
[b] Pre-extraction internal standards were outside of acceptance criteria, DEs used estimated maximum concentrations

4.3.2 Volatile emissions

The generally high DEs (>99.99%) presented in Table 20 suggest PFAS are relatively fragile, at least with respect to losing their molecular identity even at temperatures <900 °C. High DEs, however, do not necessarily ensure the absence of emissions of fluoroorganic PICs. Evacuated canisters were used to look for some known[9, 10, 42] and suspected PICs. The current method under development (now OTM-50) at the EPA can measure 30 VFCs listed in Table 21. The reporting limits for 29 of these compounds is 0.5 ppbv, while tetrafluoromethane (CF4) is limited to 50 ppbv. This method was used during the AFFF incineration experiments and the results, presented in $\mu g/m^3$, are shown in Table 21. At AFFF injection locations >1090 °C, the PIC data show very little vPFAS at the current detection limits, but as the AFFF injection temperatures fall below 1000 °C, the vPFAS increase considerably to mg/m^3 levels. The increase in VFCs also coincides with elevated CO concentrations rising from single digit levels up to ~1700 ppmv (see Table 22). Increases in CO were the result of incomplete PFAS oxidation and not associated with the natural gas combustion, as the AFFF experiments with high CO were injected post-flame long after natural gas combustion was complete.

An important finding from Table 21 is the notable emissions of relatively high concentrations (~mg/m3) of all eight 1H-perflouroalkanes (C1-C8) during the 810 °C injection experiment. These VFCs are expected to be formed during the thermolysis of the PFCAs or PFSAs under both pyrolytic and oxidative conditions.[9, 10, 38, 40, 42, 43] The fluorocarbon concentrations increase with decreasing fluoroalkyl chain length, with fluoroform (CHF_3) and pentafluoroethane (C_2HF_5) present at 810 °C, at concentrations of 7.5 and 9.0 mg/m^3, respectively. 1H-perfluorooctane (C_8HF_{17}) and 1H-perfluoroheptane (C_7HF_{15}) concentrations were significantly

lower (0.2 and 0.3 mg/m3, respectively), possibly indicating a mechanistic pathway of incremental α or β carbon removal. Tetrafluoroethylene (C_2F_4) concentrations are relatively low (~0.15 mg/m3), perhaps suggesting that a mechanism where C_2F_4 is formed[16, 44] by β carbon scission, is less important under oxidative conditions.

Note that similar results have been both experimentally and computationally derived under pyrolytic and oxidative conditions. Thermolysis often yields 1H-perfluorocarbons and 1-perfluoroalkenes with PFCAs,[9, 10, 42, 43, 45, 46] with PFSAs forming the same compounds[47] as well as perfluorocarbons.[43, 48] Computational studies predict similar products[16, 38-41] using various computational methods. All the referenced models have a lactone or sulfone intermediate with HF elimination as the first step to the loss of the functional group. After the removal of the functional group, the steps to formations of non-polar intermediates, including the breaking of carbon-carbon and carbon-fluorine bonds, are all relatively low energy steps. These steps involve unimolecular decomposition, hydrofluorination, hydrolysis, and fragmentation of the alkyl chain. A prominent and potentially important intermediate are acyl fluorides since these can readily be hydrolyzed to carboxylic acids, as suspected in this study. Altarawneh[38] examined the temperature sensitivity of PFBS destruction from 500 to 2000 K and indicated that PFBS is destroyed at low temperatures but can create fluorinated PICs at temperatures up to 1127 °C. These studies examined different conditions than the present study, but still the similarities are remarkable, and provide further support that high DEs are not necessarily indicative of the absence of PICs.

HF concentrations presented in Table 22 were not validated because no accompanying CEM measurement was available. Subsequent attempts at Method 320 validation were unsuccessful due to poor HF transport efficiencies and lack of calibration gas recoveries. These values are included for perspective to indicate approximate HF concentrations based on the amounts of AFFF introduced. Note that NO values decrease with decreasing AFFF injection temperatures. This behavior is not fully understood but may be related to selective non-catalytic reduction (SNCR) technologies used for the control of nitrogen oxides.[49-51] SNCR decreases NO concentrations in combustion effluents by reactions with added ammonia, ammonia derivatives, or urea to the combustion gases at temperatures between 700 to 1000 °C. AFFF is known to contain percent levels of amines, sulfonamides, and amides, and these may be acting to reduce the NO concentrations as the AFFF injection temperatures fall below 1000 °C. Efforts to improve confidence in FTIR measurements including HF and NO are ongoing.

Table 21. Volatile fluorinated compounds concentrations from AFFF combustion

Temperature (°C)	**Flame**	**1180**	**1090**	**970**	**870**	**810**
Canister Analytes	**(μg/m^3)**	**(μg/m^3)**	**(μg/m^3)**	**(μg/m^3)**	**(μg/m^3)**	**(μg/m^3)**
tetraflouromethane	ND	ND	ND	ND	ND	ND
hexafluoroethane	ND	ND	ND	11.4	9.36	6.51
chlorotrifluoromethane	ND	ND	ND	ND	ND	ND
fluoroform	ND	ND	ND	5.47	601	7530
octafluoropropane	ND	ND	ND	266	903	795
difluoromethane	ND	ND	ND	2.87	8.51	94.4
pentafluoroethane	0.70	1.35	0.65	3.99	276	8950
octafluorocyclobutane	ND	ND	ND	ND	ND	14.1
fluoromethane	ND	ND	ND	ND	ND	1.30

tetraflouroethylene	ND	ND	ND	ND	1.16	149
hexafluoropropylene	ND	0.19	ND	0.31	4.96	567
1,1,1-trifluoroethane	ND	ND	ND	ND	ND	ND
hexafluoropropene oxide	ND	ND	ND	ND	ND	ND
chlorodifluoromethane	ND	ND	ND	ND	ND	ND
1,1,1,2-tetrafluoroethane	ND	ND	ND	3.39	1.84	64.2
perfluorobutane	ND	0.30	ND	ND	434	620
1H heptafluoropropane	ND	0.99	ND	ND	86.8	2480
octafluourocyclopentene	ND	ND	ND	ND	5.15	235
trichlorofluoromethane	0.40	0.17	0.57	0.57	0.40	0.57
dodecafluoro-n-pentane	ND	ND	ND	ND	51.2	503
1H nonafluorobutane	ND	0.64	ND	ND	59.8	1230
tetradecafluorohexane	ND	ND	ND	ND	1.41	307
1H perflluoropentane	ND	ND	ND	ND	12.1	1000
E1*	ND	ND	ND	ND	ND	ND
hexadecaflluroheptane	ND	ND	ND	ND	ND	85.8
1H perfluorohexane	ND	ND	ND	ND	6.65	1090
perfluorooctane	ND	ND	ND	ND	ND	291
1H perfluoroheptane	ND	ND	ND	ND	ND	316
1H Perfluorooctane	ND	ND	ND	ND	ND	203
E2*	ND	ND	ND	ND	ND	ND

* E1 - Heptafluoropropyl 1,2,2,2-tetrafluoroethyl ether
* E2 - 2H-Perfluoro-5-methyl-3,6-dioxanonane

Table 22. Combustion gases during legacy AFFF combustion

Temperature (°C)	Flame	1180	1090	970	870	810
FTIR Analytes						
CO (ppm)	7.2	3.6	4.5	5.7	109	1730
CO2 (%)	6.2	6.3	5.2	5	4.4	4
HF (ppm)	427.2	340	278.3	265.8	260.1	226.6
NO (ppm)	86.7	91	63.5	38.1	4.9	0.4
SO2 (ppm)	60.9	41.7	34	31.4	35.2	35.4
Other Gas						
Oxygen, O2 (dry, %)	7.9	7.2	9	9.2	11.8	12

4.3.3 Nontargeted PFAS emissions

Additional mass spectra analysis of the OTM-45 extracts revealed there were up to 97 peaks that indicated the presence of different semivolatile polar PFAS. Figure 8 presents the sum of the peak areas for these 97 fluorinated species for the six combustion experiments and the PBT. Where the peak area of a feature was very low, an arbitrary value was given to the peak to allow

for statistical analysis by the software. This artificially makes the peak areas for fluorinated features in the blanks and some low detection samples higher than what they may actually be. Figure 8 does not correct for this, and again near blank levels may indicate the nontargeted peak areas are below detection limits. Figure 8 presents separate analysis for four OTM-45 sample fractions: front half (filter and probe rinse), back half (XAD-2 sorbent), impinger solutions, and a second volume of XAD-2 sorbent, used for these experiments, to quantify the potential for sample breakthrough. The NTA peak areas in Figure 8 are separated between those corresponding to 36 targeted PFAS (lightly shaded), and 61 nontargeted (unidentified) PFAS found. The 36 targeted PFAS are part of the other OTM-45 targeted list, and Figure 8 shows how much the total PFAS present are made up of these targeted compounds. It is apparent many of the compounds sampled during these experiments are not found in the OTM-45 list. As the temperature decreases the peak area of the OTM-45 fractions shifts from the back half XAD having the most area to the front half, or filter, fraction having the most area at 810 °C. This is due to the large increase of sulfonates in the emissions, see Table 19, that preferentially adsorbed on the filter, and to a lesser extent an increase of PFCAs on the filter too.

Figure 8 presents these data on two linear scales. The larger plot includes the 810 °C experiment, and the insert excludes these data to allow better comparison of the other experimental results. NTA indicates additional unidentified semivolatile polar PFAS mass in addition to the 36 targeted PFAS in all sample fractions. However, like the volatile non-polar PIC measurements, injection temperatures >1000 °C do not result in NTA PFAS mass significantly above blank levels. Note that the NTA also shows the suspected hysteresis effect of performing the 1180 °C experiment after the 810 °C experiment. The NTA indicates increasing PFAS emissions at AFFF injection temperatures <1000 °C, and that unidentified PFAS comprise a portion of these emissions.

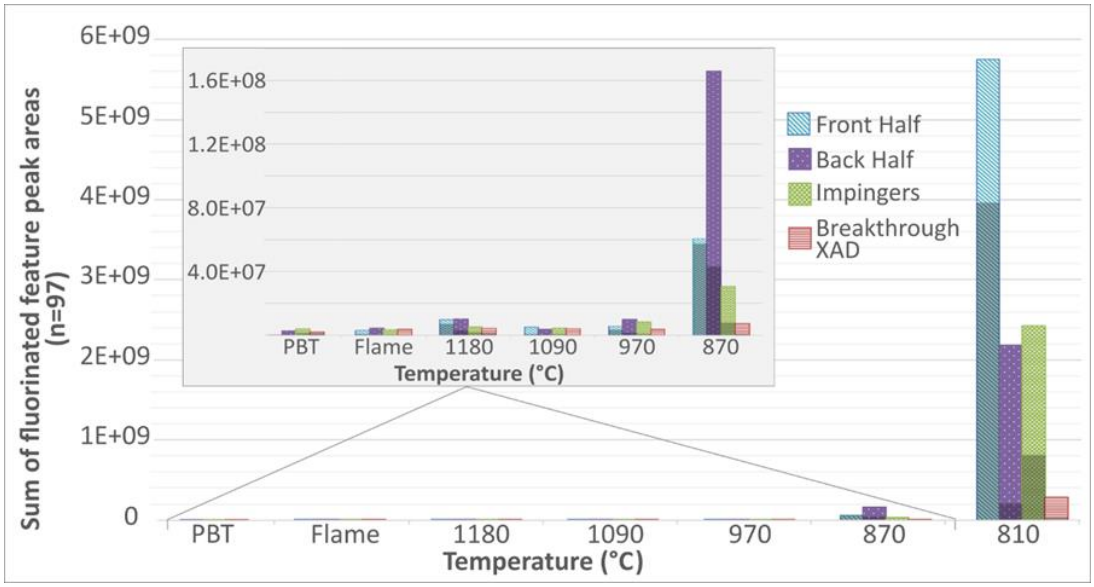

Figure 8. The sums of the peak areas of fluorinated features observed with nontargeted analyses of the OTM-45 extracts. Each fraction of the sampling train is shown for each temperature. The darkened portion of each bar is the sum of the targeted compounds' peak area.

4.4 PILOT SCALE FLUOROTELOMER BASED AFFF COMBUSTION

4.4.1 Total organic fluorine of the AFFF

The fluorotelomer based AFFF used contained few targeted PFAS at high concentrations, so organic fluorine methods were attempted to determine possible HF concentrations and an approximate concentration of PFAS in the AFFF. TOPA analysis was used to give the concentrations of the targeted PFAS and an organic fluorine value. The fluorine value from the TOPA was only 415 mg/L, much lower than it should be. This was likely due to the laboratory not using enough oxidant to oxidize all the organic compounds in the AFFF. The lab also did an AOF analysis and found about 6,000 mg/L of AOF. This is closer to the anticipated value derived from PFAS concnetrations found in literature. Literature states that the brand of AFFF used contains about 4,600 mg/L of 6:2 fluorotelomer sulfonamide alkylbetaine (6:2 FTAB) and about 2,100 mg/L of 6:2 fluorotelomer sulfonamide alkylamine (6:2 FTSaAm).[52] These compounds add an additional 3,000 mg/L of organic fluorine coming closer to the AOF value. The AOF and literature values were only semiqualitative, so a quantifiable value was not obtained. This does show that SOPs need to be revised for samples that contain high concentrations of oxidizable compounds, including PFAS and other organics.

4.4.2 Destruction of targeted PFAS

From the 28 compounds targeted in the TOPA, 12 compounds were found above the detection limit and are listed with their concentrations in Table 23. The fluorotelomer sulfonates (FTS) and PFCAs are the predominate groups of targeted compounds found in the AFFF. Due to the high dilution required for analysis, some other compounds may have been present in the AFFF. Three sulfonates, PFBS, PFHxS, and PFOS, and their detection limits are listed in Table 23 for reference.

Table 23. Targeted PFAS in fluorotelomer based AFFF

Targeted Compound	Concentration	
	mg/L	mg/g
4:2 Fluorotelomer sulfonic acid (4:2 FTS)	1.99	0.00191
6:2 Fluorotelomer sulfonic acid (6:2FTS)	23.7	0.0228
8:2 Fluorotelomer sulfonic acid (8:2 FTS)	16.7	0.0161
Perfluorobutanoic acid (PFBA)	0.946	0.000910
Perfluoropentanoic acid (PFPeA)	0.593	0.000570
Perfluorohexanoic acid (PFHxA)	10.6	0.0102
Perfluoroheptanoic acid (PFHpA)	0.399	0.000384
Perfluorooctanoic acid (PFOA)	4.08	0.00392
Perfluorononanoic acid (PFNA)*	0.161	0.000155
Perfluorodecanoic acid (PFDA)	1.57	0.00151
Perfluorododecanoic acid (PFDoA)	0.504	0.000485
Perfluorotetradecanoic acid (PFTeA)*	0.122	0.000117
Perfluorobutanesulfonic acid (PFBS)**	<0.100	<0.0000962
Perfluorohexanesulfonic acid (PFHxS)**	<0.150	<0.000144

Perfluorooctanesulfonic acid (PFOS)**	<0.100	<0.0000962

* Estimated concentration, the value is below the reporting limit and above the detection limit.
* Not detected in the sample. The values are the method detection limits.

The polar semivolatile and nonvolatile PFAS in the emissions were measured over a 3.0 h OTM-45 sample run. The total masses of the PFAS collected in the sample trains at the tested temperatures and conditions are shown in Table 24. The runs at 860 °C and above 1000 °C may be slightly biased high due to perfluoroheptanoic acid (PFHpA) being present in the method blank. The other runs below 1000 °C had concentrations of PFHpA more than ten times the method blanks' concentration, and the values will not be significantly impacted by the possible laboratory contamination. Perfluorononanoic acid (PFNA) was also present in the method blank at a level between the detection limit and the reporting limit, so the concentrations from PFNA may be slightly biased high too. The proof blank trains for OTM-45 only had 8:2 and 10:2 fluorotelomer sulfonates slightly above the detection limit, and perfluoro-3-methoxypropanoic acid was present in the method blanks. These may have only impacted the 880, 1080, and 1160 °C trains, as they had values near the detection limits for the FTS compounds and the other PFAS was not present in any sample.

Table 24. OTM-45 targeted PFAS mass per train

Temperature (°C)	**760**	**860**	**880**	**1010**	**1080**	**1160**
Injection Port	**8**	**4**	**8**	**8**	**6**	**4**
Sample volume (dscm)[a]	3.82	3.8	3.81	3.79	3.83	3.75
Compound	**ng**	**ng**	**ng**	**ng**	**ng**	**ng**
Perfluorobutanoic acid (PFBA)	36156	25.22	195.79	23.89	11.396	*<11.256*
Perfluoropentanoic acid (PFPeA)	18449	2.802	75.78	12.29	0.902	0.889
Perfluorohexanoic acid (PFHxA)	23516	4.647	178.85	21.845	1.313	1.446
Perfluoroheptanoic acid (PFHpA)[b]	4402	16.01	358.8	13.21	16.09	9.45
Perfluorooctanoic acid (PFOA)	5515	3.929	60.44	9.897	*<1.591*	1.881
Perfluorononanoic acid (PFNA)[b]	1072.9	2.07	6.34	2.347	*<1.13*	1.163
Perfluorodecanoic acid (PFDA)	1411.5	*<0.823*	11.91	2.908	*<0.652*	*<0.642*
Perfluoroundecanoic acid (PFUnDA)	277.95	*<0.888*	1.577	0.838	*<0.662*	*<0.653*
Perfluorododecanoic acid (PFDoDA)	415.7	*<0.4647*	3.573	1.13	*<0.375*	*<0.3691*
Perfluorotridecanoic acid (PFTriDA)	85.05	*<0.67*	0.589	*<0.55*	*<0.547*	*<0.537*
Perfluorotetradecanoic acid (PFTeDA)	126.75	*<0.898*	1.037	*<0.738*	*<0.733*	*<0.611*
Perfluorohexadecanoic acid (PFHxDA)	90.69	*<1.208*	*<0.968*	*<1*	*<1.002*	*<0.984*
Perfluorobutanesulfonic acid (PFBS)	*<67.7*	2.066	*<1.532*	*<1.545*	*<1.543*	*<1.523*
Perfluorohexanesulfonic acid (PFHxS)	*<42.55*	1.303	0.983	0.543	0.562	*<0.534*
Perfluorooctanesulfonic acid (PFOS)	53.65	11.106	3.727	0.962	0.907	*<0.778*
1H,1H,2H,2H-Perfluorohexanesulfonic acid (4:2 FTS)	36.72	*<0.3558*	*<0.311*	*<0.328*	*<0.325*	*<0.3193*
1H,1H,2H,2H-Perfluorooctanesulonic acid (6:2 FTS)	1391.6	*<21.68*	*<13.074*	*<13.113*	*<13.107*	*<13.016*
1H,1H,2H,2H-Perfluorodecanesulfonic acid (8:2 FTS)	459.4	*<0.77*	2.024	1.105	*<0.685*	0.863

1H,1H,2H,2H-Perfluorododecanesulfonic acid (10:2 FTS)	231.15	*<0.914*	1.05	*<0.813*	*<0.808*	*<0.794*
2H,2H-Perfluorooctanoic acid (6:2 FTCA)	1102.4	*<3.144*	*<2.246*	*<2.33*	*<2.318*	*<2.286*
2H,2H-Perfluorodecanoic acid (8:2 FTCA)	474.65	*<1.886*	*<1.614*	*<1.705*	*<1.692*	*<1.659*
2H,2H-Perfluorododecanoic acid (10:2 FTCA)	231.7	*<2.175*	*<1.756*	*<1.84*	*<1.828*	*<1.796*
2H-Perfluoro-2-octenoic acid (6:2 FTUCA)	595.2	*<0.754*	1.069	*<0.61*	*<0.606*	*<0.596*
2H-Perfluoro-2-decenoic acid (8:2 FTUCA)	286.64	*<1.097*	1.153	*<1.02*	*<1.012*	*<0.992*
Total PFAS	96491.9	106.880	926.193	116.557	61.786	55.037

Italics - All train fractions were below the MDL. The value listed is the MDL value.

a - dry standard cubic meter (dscm)

b - Compound found in laboratory method blank

The sample volume, percent water, mass per train values for the PFAS detected in the AFFF concentrate were used to determine the DEs for the measured PFAS, see Table 25. The DE was calculated using equation 5 from the Federal Register for calculating DRE.[53]

$$DE\ (\%) = \left(\frac{W_{in} - W_{out}}{W_{in}}\right) \times 100\% \qquad 5$$

Where W_{in} is the mass of the PFAS fed, and W_{out} is the mass of the PFAS in the exhaust. The low concentrations of targeted PFAS in the AFFF limits the number of nines that can be computed for the PFAS. High destruction of the parent PFAS molecule can be seen though.

Table 25. Destruction Efficiencies for targeted PFAS

Temperature (°C)	**760**	**860**	**880**	**1010**	**1080**	**1160**
Compound	**DE (%)**	**DE (%)**	**DE (%)**	**DE (%)**	**DE (%)**	**DE (%)**
4:2 Fluorotelomer sulfonic acid (4:2 FTS)	99.9665	99.9997	99.9997	99.9997	99.9997	99.9997
6:2 Fluorotelomer sulfonic acid (6:2FTS)	99.8933	99.9983	99.9990	99.9991	99.9990	99.9990
8:2 Fluorotelomer sulfonic acid (8:2 FTS)	99.9500	99.9999	99.9998	99.9999	99.9999	99.9999
Perfluorobutanoic acid (PFBA)	30.5179	99.9511	99.6194	99.9595	99.9782	99.9787
Perfluoropentanoic acid (PFPeA)	43.4410	99.9913	99.7650	99.9668	99.9972	99.9973
Perfluorohexanoic acid (PFHxA)	95.9669	99.9992	99.9690	99.9967	99.9998	99.9998
Perfluoroheptanoic acid (PFHpA)[a]	79.9432	99.9265	98.3462	99.9469	99.9271	99.9576
Perfluorooctanoic acid (PFOA)	97.5426	99.9982	99.9728	99.9961	99.9993	99.9992
Perfluorononanoic acid (PFNA)[a]	87.8852	99.9764	99.9276	99.9766	99.9873	99.9871
Perfluorodecanoic acid (PFDA)	98.3656	99.9990	99.9860	99.9970	99.9992	99.9993
Perfluorododecanoic acid (PFDoA)	98.9974	99.9983	99.9870	99.9964	99.9987	99.9987
Perfluorotetradecanoic acid (PFTeA)	98.1113	99.9865	99.9844	99.9903	99.9891	99.9910

a – compound was present in the laboratory method blank

4.4.3 Nonpolar volatile fluorinated compounds in the emissions

To help determine the mineralization of the PFAS in the AFFF by identifying common PICs, OTM-50 was used to analyze for volatile nonpolar VFCs. The results of the analyses are shown in Table 26. The nitrogen blank for the experiments had octafluoropropane, hexafluoropropene, decafluorobutane, trichlorofluoromethane, and 1H-perfluorobutane at levels

slightly above the detection limit. Any sample that had concentrations of these compounds above the reporting limit has concentrations greater than ten times the blank levels, so the data is not impacted. Samples with concentrations between the method detection limit and the reporting limit may provide values that are biased high. Duplicate samples at 760 and 1160 °C were taken to test the measurement repeatability, the values good repeatability, the data is shown in Appendix A, Table A1.

Table 26. OTM-50 results for the fluorotelomer AFFF incineration

Injection composition	**AFFF only**					
Temperature (°C)	**760**	**860**	**880**	**1010**	**1080**	**1160**
Injection Port	**8**	**4**	**8**	**8**	**6**	**4**
Compounds	μg/m^3	μg/m^3	μg/m^3	μg/m^3	μg/m^3	μg/m^3
Tetrafluoromethane	BDL	BDL	BDL	BDL	*2.37*	BDL
Hexafluoroethane	11.25	33.99	44.34	*2.62*	*1.01*	BDL
Chlorotrifluoromethane	*1.94*	4.91	5.17	*0.26*	BDL	BDL
Trifluoromethane	1187	5.72	12.77	4.51	*0.60*	BDL
Octafluoropropane	40.65	56.55	55.86	BDL	BDL	BDL
Difluoromethane	2.44	BDL	BDL	*0.20*	BDL	BDL
1,1,1,2,2-Pentafluoroethane	417.0	*0.59*	2.61	*2.28*	BDL	BDL
1,1,2,2,3,3,4,4-Octafluorocyclobutane	BDL	BDL	BDL	BDL	BDL	BDL
Fluoromethane	BDL	BDL	BDL	BDL	BDL	BDL
Tetrafluoroethylene	22.74	BDL	*0.24*	BDL	BDL	BDL
Hexafluoropropene	10.57	*0.37*	*0.36*	*0.38*	BDL	BDL
1,1,1-trifluoroethane	5.30	BDL	BDL	BDL	BDL	BDL
Hexafluoropropene Oxide	BDL	BDL	BDL	BDL	BDL	BDL
Chlorodifluoromethane	BDL	*0.32*	*0.21*	*0.44*	BDL	*0.21*
1,1,1,2-Tetrafluoroethane	BDL	*0.63*	*0.37*	*0.39*	BDL	BDL
Decafluorobutane	42.06	*2.06*	*1.72*	BDL	BDL	BDL
1,1,1,2,2,3,3-Heptafluoropropane	59.87	BDL	*0.82*	*0.86*	BDL	BDL
Octafluorocyclopentene	BDL	BDL	BDL	BDL	BDL	BDL
Trichlorofluoromethane	BDL	*0.68*	*0.50*	*0.69*	BDL	*0.34*
Dodecafluoro-n-pentane	6.05	BDL	BDL	1.46	BDL	BDL
1,1,1,2,2,3,3,4,4-Nonafluorobutane	57.91	BDL	*0.80*	0.83	BDL	BDL
Tetradecafluorohexane	BDL	BDL	BDL	BDL	BDL	BDL
1,1,1,2,2,3,3,4,4,5,5-Undecafluoropentane	32.36	BDL	BDL	2.39	BDL	BDL
Heptafluoropropyl 1,2,2,2-tetrafluoroethyl ether	BDL	BDL	BDL	BDL	BDL	BDL
Hexadecafluoroheptane	BDL	BDL	BDL	BDL	BDL	BDL
1,1,1,2,2,3,3,4,4,5,5,6,6-Tridecafluorohexane	32.43	BDL	BDL	BDL	BDL	BDL
Octadecafluorooctane	BDL	BDL	BDL	BDL	BDL	BDL
1,1,1,2,2,3,3,4,4,5,5,6,6,7,7-Pentadecafluoroheptane	BDL	BDL	BDL	BDL	BDL	BDL
1,1,1,2,2,3,3,4,4,5,5,6,6,7,7,8,8-Heptadecafluorooctane	21.80	BDL	BDL	BDL	BDL	BDL
2H-Perfluoro-5-methyl-3,6-dioxanonane	BDL	BDL	BDL	BDL	BDL	BDL

BDL: below the detection limit

italics: below the reporting limit but above the detection limit

At the 760 ℃ the most abundant VFC PIC is trifluoromethane, 1.2 mg/m^3, with the other 1H-perfluorocarbons present. As the temperature increases to 860 and 880 ℃, the more stable perfluorocarbons become more abundant, with octafluoropropane and hexafluoroethane being the most concentrated. As the temperature increases over 1000 ℃, mainly C1 and C2 species are seen. Tetrafluoromethane is the main compound at 1080 ℃, but it and hexafluoroethane are both below the reporting limits. The 1160 ℃ run has no compounds found over the reporting limit and only has two chlorinated compounds that are often in the laboratory background and blanks. As the temperatures approach and exceed 1100 ℃ there are nearly no measurable VFC PICs.

The OTM-50 data shows that the DE of the parent PFAS is not a good metric to indicate that mineralization has occurred. The AFFF injections at 860 ℃ at port 4 and at 880 ℃ at port 8 have very different concentrations of the parent PFAS on the trains despite the main difference being almost a second longer residence time for the 860 ℃ injection at port 4. The 880 ℃ run at port 8 had about nine times more PFAS mass collected on the OTM-45 train than the 860 ℃ run at port 4. The 860 ℃ run's PFAS mass was closer to the runs over 1000 ℃ than the run near the same temperature. The OTM-50 data is important. For the 860 ℃ and 880 ℃ runs the VFC concentrations are similar, where the most concentrated compound, octafluoropropane, only having a 0.69 μg/m^3 difference between the runs. The amount of the VFCs formed is more dependent on temperature than residence time.

4.4.4 Hexafluoroethane co-injection with AFFF

Previous studies (Sections 4.1, 4.2, and 4.3) relied on FTIR for the measurement of C_2F_6 and used the data collected from injecting only the pure gas into the furnace. Here OTM-50 was used to analyze the emissions from the injection of a mixture of C_2F_6 and AFFF to the furnace. OTM-50 lowers the previous FTIR detection limits by at least two orders of magnitude and allows for the observation of other potential low concentration PICs. Adding the gas to the AFFF feed makes the C_2F_6 experience conditions more representative of the PFAS in the AFFF.

The experiments' OTM-50 concentrations, C_2F_6 DE, and mineralization efficiency (ME) are shown in Table 27. Since the runs at 860 and 880 °C showed low destruction, co-injection at 760 °C was not carried out. The DEs were calculated using the equation 5. The MEs were estimated by adding the mass of the molar equivalent of C_2F_6 equal to the amount of CF_4 present, two moles of CF_4 are equivalent to one mole of C_2F_6. The formation of CF_4 as a PIC was observed by OTM-50 in these tests. The formation of CF_4 and the low μg/m^3 concentrations of C_2F_6 have not previously been observed with the FTIR. The concentrations derived from the FTIR analyses were below the detection limit for the temperatures above 1000 °C, showing the value of OTM-50. The 860 and 880 ℃ runs required large dilutions to measure the C_2F_6, so the other VFCs were not observed.

Table 27. OTM-50 results for hexafluoroethane co-injection with AFFF

Temperature (°C)	CF_4 (μg/m3)	C_2F_6 (μg/m3)	C_2F_6 DE (%)	ME (%)
860	BDL	117600	41.46	41.46*
880	BDL	187100	6.87	6.87*
1010	16.44	6750	96.64	96.63

1080	338.13	149.4	99.93	99.66
1160	163.68	33.43	99.98	99.86

* Sample was diluted, so the detection limits were raised for the other compounds and no other compounds were detected

The destruction of C_2F_6 shows over 99.9% destruction as the temperature approaches 1100 °C. This is the same range the AFFF only injections had near detection limit amounts of both PFAS and nonpolar VFC concentrations. This supports using C_2F_6 as a principle component for a trial burn at a facility that desires to treat high concentration PFAS matrices, as laid out in the EPA's Interim Guidance for Destruction and Disposal of PFAS.[54] This study is only at pilot scale and the results may not correlate to a full scale system. Testing a full scale site is needed to verify that the high destruction of PFAS and absence of VFC PICs correlates to a high C_2F_6 DE.

4.4.5 Analysis of semivolatile organic compounds

The incineration of nonhazardous and hazardous wastes can form semivolatile PICs of concern, such as chlorinated dioxins and polycyclic aromatic hydrocabons (PAHs). It is unknown if incinerating PFAS can create fluorinated equivalents or if fluorine can enhance the formation of these PICs by scavenging available radicals. Currently, there are no methods to find these types of fluorinated molecules. The EPA is looking to modify Methods 0010 and 8270 to attempt to identify these compounds, if present. Several other types of PFAS could also fall into this category of nonpolar semivolatile compounds, such as perfluorosulfonamide based compounds, fluorotelomer alcohols, and long chain perfluorocarbons.

To help develop this method, Method 0010 was run, the trains extracted with methylene chloride, and Method 8270 was run with the extra tentatively identified compounds (TICs) analysis performed by the lab. The goal was to attempt to identify any semivolatile fluorinated species that may be present. This method will likely be developed into another OTM in the future, once a target list is developed.

During this test, the Method 8270 runs showed virtually no compounds above the detection limit. The only compounds seen were common XAD degradation compounds, such acetophenone and phenol, near the detection limit. There was one fluorinated compound detected for all the runs, 2-fluorobiphenyl found in the 860 °C run. 2-fluorobiphenyl was above the reporting limit at 129 μg/train. This was only seen once and cannot be verified as a PIC.

The TICs analysis showed several compounds in each run, but none were obviously fluorinated. The data from the analyses is attached at the end of this report for further review. More work is needed to determine how many of the species ionize and behave in the GC/MS method. Then, better workflows can be established to attempt to determine the presence of fluorinated compounds.

5.0 CONCLUSIONS AND IMPLICATIONS FOR FUTURE RESEARCH / IMPLEMENTATION

5.1 BENCH SCALE PERFLUOROCARBON THERMAL DESTRUCTION

The thermal treatment profiles of five C1 – C5 FCs, CF_4, C_2F_6, C_3F_8, C_4F_{10}, and C_5F_{12} were investigated using the bench scale system both in the air and N_2 environments. The effluent gases from the furnaces were analyzed for the parent compounds, HF, PICs/PIDs, moisture and CO_2 using FTIR. The parent compound DE, ME, and fluorine (F) mass balance were also calculated and presented. The parent compounds' DEs were obtained; however, the ME and F mass balances were less reliable. The destruction efficiencies were approximately between 40 and 60% range at the high temperature where the complete parent compound destruction was observed. The F mass balances were as low as 35% up to 70% at the high temperature. The low ME and F mass balance were likely due to the gas-surface reaction between parent compound/PIDs/HF and either alumina or fused silica quartz reactor wall. These complications with determining ME cause ME not to be a relevant metric to evaluate the mineralization of PFAS in these experiments. The DE and the presences of PIDs can provide a better indication of destruction. The major PIDs observed were CF_2O, CF_3H, and C_2F_6. CF_2O was formed more in the air environment, and CF_3H and C_2F_6 were formed mostly in the N_2 environment.

The extreme stability of the carbon-fluorine bonds in CF_4 was shown by it's DE and ME profiles. The condition to decompose CF_4 over 99% was a temperature of 1600 °C and a residence time of 1 s. That for C_2F_6 and C_3F_8 were 1000°C 4 s and 850 °C 8 s, respectively. That for C_4F_{10} and C_5F_{12} was 850 °C and 2 s. The temperature of 850 °C and the residence time of 2 s was the lowest temperature and the shortest residence time; therefore, they can be decomposed over 99% at the lower temperature or shorter residence time. This implies that C_2F_6 may be the best PFC to use as a potential mineralization indicator compound or surrogate for PFAS destruction.

5.2 PILOT SCALE PERFLUOROCARBON THERMAL DESTRUCTION

Experimental results indicate that CF_4 is the most difficult to destroy of the tested compounds with DEs of only ~90% when introduced through the 45 kW flame (~1295 °C/2363 °F peak bulk gas temperature) and <14% when introduced post-flame (<1295 °C/2363 °F). Increasing the furnace load (64 kW), and peak bulk gas temperature (~1400 °C/2552 °F), increased CF_4 DE through the flame (~95%). However, DEs for CF_4 introduced with the combustion air were lower (~89%), suggesting the opportunity for CF_4 to partially bypass the flame. Small CF_4 DEs measured at moderate and low temperatures, may be the result of catalytic reactions with alumina-rich high temperature refractory surfaces within the furnace or spectral interference. These results suggest that CF_4 may not be a very useful indicator of the destruction of PFAS but may be useful to determine the relative thermal exposures of PFAS treated by different incinerators and introduced at different locations and as a tracer gas to ensure the injection system works.

The presence of C-H and C-C bonds in these PFAS molecules greatly affected the DEs. For CHF_3, DEs of >99% were measured even when introduced well downstream of the flame (~930 °C). C_2F_6 was somewhat more difficult to destroy, but still exhibited DEs >99% in the flame and through 1060 °C post-flame locations. Since most PFAS of practical interest contain C-C bonds, these initial results for C_2F_6 suggest that PFAS can be destroyed when subjected to reasonably aggressive thermal environments that include free radical flame chemistry. This suggests that C_2F_6 may be an effective indicator of PFAS destruction and a potential surrogate.

This study successfully demonstrated the feasibility of using FTIR as a CEM capable of measuring multiple gas-phase species (including some fluorocarbons) extracted from the combustion flue gases. Real-time FTIR-based PIC measurements were able to characterize the presence of several fluoro-organic species in the combustion flue gases including C_2F6, and CF_4 at operationally relevant concentrations, as well as conventional flue gas constituents like CO, CO_2, water vapor, and HF. For the most part, PICs were identified during experiments when the PFAS was introduced at lower temperatures downstream from the flame. However, the relatively lower energies associated with C-C and C-H bond, which is particularly susceptible to hydrogen abstraction by OH radicals, suggest the possibility of the formation of CF_2 and CF_3 radicals at thermal conditions that are unable to fully de-fluorinate these species resulting in fluorinated PIC formation.

Finally, even when experimental measurements indicate DEs >99%, FTIR measurements of HF agreed poorly with expected concentrations. A significant factor may be due to fluorine or HF adsorption, reaction, or loss to refractory and other combustor surfaces. Fluorine reaction with the silica (Si) present in most refractories (producing vapor-phase SiF_4) is a known issue[55], and the cause of many instances of refractory failure in incinerator systems. This shows that as the scale of the system increases there is less possibility of fluorine mass balance and that the most important metric for PFAS destruction is the absence of PICs or PIDs.

5.3 PILOT SCALE LEGACY AFFF COMBUSTION

Some PFAS, and perhaps most PFAS of industrial importance, seem to be simultaneously both fragile and stable, and the simple use of DEs as the sole indicator of complete PFAS destruction may be misleading. For some PFAS, relatively low energies are needed to remove the polar functional group, with the first step being the loss of the terminal C or S likely through a lactone or sulfone intermediate, leaving a non-polar fluoroalkyl chain. If conditions prevent continuation of the destruction mechanisms, this may result in high DEs, >99.99%, but not necessarily the mineralization of the PFAS molecule. Here, complete destruction is defined as mineralization, which for a C, F, O, H system results in CO_2, HF, and H_2O. In these experiments, combustion conditions were examined that produced high DEs and measurable PICs. However, when AFFF was exposed to temperatures ≥1080 °C (including exposure to flames and near adiabatic flame temperatures) high DEs and no measured VFC PICs were observed. Based on these experiments, high destruction of PFAS can be shown only by considering both high DEs and the absence of PICs.

Finally, note that these experiments focused on steady-state combustor operations. This was done to simplify the fluid dynamics and mixing behavior and allow focus on kinetic aspects. However, except for thermal oxidizers and some other unique applications, HWIs (often rotary kilns) introduce wastes in multiple ways, including batch solids and contained liquids. These cause transient release of organics to the vapor phase that may temporarily overwhelm available oxygen and depress temperatures. For most HWIs, the afterburner is intended to dampen and smooth this transient behavior, but it is likely that the time dependent behavior of PFAS in HWIs and other batch fed system will depend on the system's ability to smooth these transients and maintain high temperatures. More research into rotary kiln systems and full-scale incinerators is needed.

5.4 PILOT SCALE FLUOROTELOMER AFFF

The incineration of a fluorotelomer based AFFF showed essentially the same results as the perfluorinated based AFFF. The predominant PICs formed consisted of perfluorocarbons, 1H-perfluorocarbons, and PFCAs. The fluorotelomer sulfonates that were most abundant in the targeted analysis of the AFFF, were destroyed at low temperatures, but the VFCs identified by OTM-50 and other PFAS did not approach the detection limit or blank levels until the temperature approached 1100 °C. Above 1080 °C the PFAS DEs were very high, the VFCs below the reporting limit, and the destruction of hexafluoroethane was above 99%. This data supports the perfluorinated AFFF study, showing promising correlations between the destruction of C_2F_6 and the absence of PICs.

The impact of residence time was looked at here too. An injection at 860 °C with a slightly longer residence time than another injection at 880°C showed less PFAS on the OTM-45 train and higher DEs. OTM-50 results were similar though, potentially indicating that the residence time has little to do with the VFC PICs formed. More research is needed, but this does emphasize the importance of testing each incinerator and not relying on the PFAS DEs as the metric for successful mineralization.

5.5 CONCLUSION AND FUTURE DIRECTION

5.5.1 PICs formed during AFFF incineration

A research objective was to attempt to identify PICs that are formed when incomplete mineralization of PFAS occurs. It was found that nonpolar VFCs found in OTM-50 were common PICs identified in the emissions from PFCs, legacy perfluorinated, and fluorotelomer based AFFFs. At temperatures below 800 °C, homologous series of perfluorocarbons and 1H-perfluorocarbons from C1 to C8 were prevalent. As the temperatures approached 1000 °C, shorter chain VFCs became the most abundant with C2 and C3 perfluorocarbons dominating the PICs. Between 1000 and 1100 °C C_2F_6 and CF_4 were often the only major VFCs present. Over 1100 °C essentially no VFCs were measured.

During the AFFF experiments, it became apparent that PFCAs were also formed as PICs. The DEs for the PFCAs were higher than the PFSAs, which is contrary to the groups' stabilities. This indicates, as with other models and methods, that in the oxidizing environment with high concentrations of water present, PFCAs are readily formed during the destruction process. This is an area where more research could be interesting to help aid with groups that are attempting to determine mechanisms and models for PFAS destruction.

5.5.2 Conditions demonstrating low PICs and high DEs

What furnace conditions that may result in minimal or no PICs and high DEs of PFAS was an objective of this project. From the bench scale perfluorocarbon tests to pilot scale AFFF tests, it is apparent that high DEs can occur with fairly low temperatures. However, to effectively mineralize the PFAS and ensure minimal PICs or PFAS emissions, it was found that temperatures near or above 1100 °C may be required. This is only based the pilot scale tests with AFFF as the matrix, so it is not necessarily applicable to full scale systems that are much more complex.

The presence of flame or other radicals from other compounds in AFFF being destroyed may help with the mineralization of PFAS. The introduction of PFAS with radicals and other

organic compounds can change the incineration conditions and may impact PFAS and PFC destruction. More complex waste feeds than used here, may have more available hydrogen radicals or reactive species that may aid in the mineralization of PFAS. It may be possible that the measured temperature could be lower, but with the flame exposure, or the presence of other species, the destruction is still high. This is where full-scale testing in the future is important.

5.5.3 Potential PFAS destruction indicators

A research objective was to determine if there is a practical metric of PFAS mineralization, such as a potential indicator of destruction or surrogate that can represent a larger class of PFAS. At small scale and pilot scale, the destruction of C_2F_6 is consistent with the destruction of the PFAS and the absence of PICs. Appendix A in the recent PFAS Destruction and Disposal Guidance[54] provides an outline of a performance test for a PFAS treatment facility. Following the procedures from trial burns, the Guidance recommends comprehensive emissions characterization along with the destruction of C_2F_6 or CF_4. More data is needed to determine any correlation between the DEs and high mineralization, high PFAS destruction and the absence of PICs. Future work at full scale facilities burning typical waste streams is needed to help determine the correlation between indicator/surrogate destruction and PFAS mineralization, if any.

5.5.4 Future work

This project was performed at a pilot scale incinerator that is closer to a thermal oxidizer, with very stable and uniform temperatures and conditions, than most commercial hazardous waste facilities. It is vital to perform similar source emissions characterizations and indicator injections at full scale facilities. Full-scale incinerators would have a more complex matrix being incinerated along with the PFAS laden materials. Full-scale incinerators can have more mixing, uneven hot and cool zones, longer residence times, more flame exposure, and other differences from the simplified pilot scale furnace used here. These differences could impact PFAS destruction, causing higher or lower amounts of mineralization. These differences make full-scale testing a high priority, as the conditions needed for mineralization will likely be different in each facility. This could impact the amount of PICs and also the destruction of the indicator gases, hexafluoroethane and tetrafluoromethane. Full-scale studies are needed to determine if a potential correlation between their destruction and the presence of PICs exists.

It is critical to investigate the emissions from the incineration of representative waste streams which include chlorinated wastes with the PFAS, as well as other halogenated (bromine containing) wastes in future testing at full scale and pilot scale incinerators. Halogenated wastes are known to aid in the molecular growth of PICs and produce highly toxic species like chlorinated dioxins and the like. It is important to verify if mixed fluoro/chloro wastes produce any similar products, or if the fluorine enhances the synthesis of nonfluorinated compounds of concern. Also, the more complicated matrix typically incinerated in hazardous waste incinerators may impact the destruction of the indicator gases, so more data about their destruction in complex matrices is needed. This data is needed to help determine correlations between the presence of PICs and the destruction of perfluorocarbon indicator gases.

Moreover, it is critical to identify the PICs/PIDs associated with these more representative waste streams. In association with this critical need, the characterization of semi-volatile and non-volatile nonpolar PICs/PICs is most important, as this chemical class of compounds has the potential to have the greatest health concerns, if emitted. In addition, these comprehensive

PICs/PIDs characterizations are integral to the development and establishment of appropriate target analyte lists.

6.0 LITERATURE CITED

1. Prevedouros, K.; Cousins, I. T.; Buck, R. C.; Korzeniowski, S. H., Sources, fate and transport of perfluorocarboxylates. *Environ Sci Technol* **2006,** *40*, (1), 32-44. DOI: 10.1021/es0512475
2. Ghisi, R.; Vamerali, T.; Manzetti, S., Accumulation of perfluorinated alkyl substances (PFAS) in agricultural plants: A review. *Environ Res* **2019,** *169*, 326-341. DOI: 10.1016/j.envres.2018.10.023
3. Cordner, A.; De La Rosa, V. Y.; Schaider, L. A.; Rudel, R. A.; Richter, L.; Brown, P., Guideline levels for PFOA and PFOS in drinking water: the role of scientific uncertainty, risk assessment decisions, and social factors. *J Expo Sci Environ Epidemiol* **2019,** *29*, (2), 157-171. DOI: 10.1038/s41370-018-0099-9
4. Haukas, M.; Berger, U.; Hop, H.; Gulliksen, B.; Gabrielsen, G. W., Bioaccumulation of per- and polyfluorinated alkyl substances (PFAS) in selected species from the Barents Sea food web. *Environ Pollut* **2007,** *148*, (1), 360-71. DOI: 10.1016/j.envpol.2006.09.021
5. Pan, Y.; Zhang, H.; Cui, Q.; Sheng, N.; Yeung, L. W. Y.; Guo, Y.; Sun, Y.; Dai, J., First Report on the Occurrence and Bioaccumulation of Hexafluoropropylene Oxide Trimer Acid: An Emerging Concern. *Environ Sci Technol* **2017,** *51*, (17), 9553-9560. DOI: 10.1021/acs.est.7b02259
6. Lemal, D. M., Perspective on fluorocarbon chemistry. *J Org Chem* **2004,** *69*, (1), 1-11. DOI: 10.1021/jo0302556
7. Qin, L.; Han, J.; Wang, G.; Kim, H. J.; Kawaguchi, I., Highly Efficient Decomposition of CF4 Gases by Combustion. *Conference on Environmental Pollution and Public Health* **2010**, 126-130. DOI:
8. Han, S.-H.; Park, H.-W.; Kim, T.-H.; Park, D.-W., Large Scale Treatment of Perfluorocompounds Using a Thermal Plasma Scrubber. *Clean Technology* **2011,** *17*, (3), 250-258. DOI: 10.7464/ksct.2011.17.3.250
9. Krusic, P. J.; Marchione, A. A.; Roe, D. C., Gas-phase NMR studies of the thermolysis of perfluorooctanoic acid. *J. Fluor. Chem.* **2005,** *126*, (11-12), 1510-1516. DOI: 10.1016/j.jfluchem.2005.08.016
10. Krusic, P. J.; Roe, D. C., Gas-phase NMR technique for studying the thermolysis of materials: thermal decomposition of ammonium perfluorooctanoate. *Anal Chem* **2004,** *76*, (13), 3800-3. DOI: 10.1021/ac049667k
11. Tsang, W.; Burgess, D. R.; Babushok, V., On the Incinerability of Highly Fluorinated Organic Compounds. *Combust. Sci. Technol.* **1998,** *139*, (1), 385-402. DOI: 10.1080/00102209808952095
12. Other Test Method 45 (OTM-45) Measurement of Selected Per- and Polyfluorinated Alkyl Substances from Stationary Sources. https://www.epa.gov/sites/default/files/2021-01/documents/otm_45_semivolatile_pfas_1-13-21.pdf, Accessed September 8, 2022, U.S. EPA 2021
13. Other Test Method 50 (OTM-50) Sampling and Analysis of Volatile Fluorinated Compounds from Stationary Sources Using Passivated Stainless-Steel Canisters. https://www.epa.gov/system/files/documents/2024-01/otm-50-release-1_0.pdf, Accessed January 17, 2024, U.S. EPA 2024

14. Wang, F.; Lu, X.; Li, X. Y.; Shih, K., Effectiveness and Mechanisms of Defluorination of Perfluorinated Alkyl Substances by Calcium Compounds during Waste Thermal Treatment. *Environ Sci Technol* **2015,** *49*, (9), 5672-80. DOI: 10.1021/es506234b
15. Aleksandrov, K.; Gehrmann, H. J.; Hauser, M.; Matzing, H.; Pigeon, D.; Stapf, D.; Wexler, M., Waste incineration of Polytetrafluoroethylene (PTFE) to evaluate potential formation of per- and Poly-Fluorinated Alkyl Substances (PFAS) in flue gas. *Chemosphere* **2019,** *226*, 898-906. DOI: 10.1016/j.chemosphere.2019.03.191
16. Altarawneh, M., A theoretical study on the pyrolysis of perfluorobutanoic acid as a model compound for perfluoroalkyl acids. *Tetrahedron Lett.* **2012,** *53*, (32), 4070-4073. DOI: 10.1016/j.tetlet.2012.05.109
17. McCord, J.; Strynar, M., Identification of Per- and Polyfluoroalkyl Substances in the Cape Fear River by High Resolution Mass Spectrometry and Nontargeted Screening. *Environ Sci Technol* **2019,** *53*, (9), 4717-4727. DOI: 10.1021/acs.est.8b06017
18. Newton, S.; McMahen, R.; Stoeckel, J. A.; Chislock, M.; Lindstrom, A.; Strynar, M., Novel Polyfluorinated Compounds Identified Using High Resolution Mass Spectrometry Downstream of Manufacturing Facilities near Decatur, Alabama. *Environ Sci Technol* **2017,** *51*, (3), 1544-1552. DOI: 10.1021/acs.est.6b05330
19. Dellinger, B.; Hall, D. L., The Viability of Using Surrogate Compounds for Monitoring the Effectiveness of Incineration Systems. *Journal of the Air Pollution Control Association* **1986,** *36*, (2), 179-183. DOI: 10.1080/00022470.1986.10466059
20. Shah, J. K., Surrogate burns in deactivation furnace system. *J Hazard Mater* **1999,** *66*, (3), 279-90. DOI: 10.1016/s0304-3894(99)00014-x
21. U. S. Environmental Protection Agency. Fluorinated Greenhouse Gas Production: Monitoring and QA/QC Requirements, Destruction device performance testing. 40 CFR 98.124(g), **2024**.
22. Krug, J. D.; Lemieux, P. M.; Lee, C. W.; Ryan, J. V.; Kariher, P. H.; Shields, E. P.; Wickersham, L. C.; Denison, M. K.; Davis, K. A.; Swensen, D. A.; Burnette, R. P.; Wendt, J. O. L.; Linak, W. P., Combustion of C1 and C2 PFAS: Kinetic modeling and experiments. *J Air Waste Manag Assoc* **2022,** *72*, (3), 256-270. DOI: 10.1080/10962247.2021.2021317
23. Steinmetz, S. A.; Herrington, J. S.; Winterrowd, C. K.; Roberts, W. L.; Wendt, J. O. L.; Linak, W. P., Crude glycerol combustion: Particulate, acrolein, and other volatile organic emissions. *Proceedings of the Combustion Institute* **2013,** *34*, (2), 2749-2757. DOI: https://doi.org/10.1016/j.proci.2012.07.050
24. Yoo, J. I.; Shinagawa, T.; Wood, J. P.; Linak, W. P.; Santoianni, D. A.; King, C. J.; Seo, Y. C.; Wendt, J. O., High-temperature sorption of cesium and strontium on dispersed kaolinite powders. *Environ Sci Technol* **2005,** *39*, (13), 5087-94. DOI: 10.1021/es048064n
25. Linak, W. P.; Miller, C. A.; Wood, J. P.; Shinagawa, T.; Yoo, J.-I.; Santoianni, D. A.; King, C. J.; Wendt, J. O. L.; Seo, Y.-C., High Temperature Interactions Between Residual Oil Ash and Dispersed Kaolinite Powders. *Aerosol Sci. Technol.* **2004,** *38*, (9), 900-913. DOI: 10.1080/027868290500805
26. Method 533 - Determination of Per- and Polyfluoroalkyl Substances in Drinking Water by Isotope Dilution Anion Exchange Solid Phase Extraction and Liquid Chromatography/Tandem Mass Spectrometry. https://www.epa.gov/sites/default/files/2019-12/documents/method-533-815b19020.pdf, Accessed September 13, 2022, U.S. EPA 2019

27. Linak, W. P.; Srivastava, R. K.; Wendt, J. O. L., Metal Aerosol Formation in a Laboratory Swirl Flame Incinerator. *Combust. Sci. Technol.* **1994,** *101*, (1-6), 7-27. DOI: 10.1080/00102209408951863
28. Method 19 - Determination of Sulfur Dioxide Removal Efficiency and Particulate, Sulfur Dioxide, and Nitrogen Oxide Emission Rates. https://www.epa.gov/sites/default/files/2017-08/documents/method_19.pdf, Accessed September 13, 2022, U.S. EPA 2017
29. Shields, E. P.; Krug, J. D.; Roberson, W. R.; Jackson, S. R.; Smeltz, M. G.; Allen, M. R.; Burnette, R. P.; Nash, J. T.; Virtaranta, L.; Preston, W.; Liberatore, H. K.; Wallace, M. A. G.; Ryan, J. V.; Kariher, P. H.; Lemieux, P. M.; Linak, W. P., Pilot-Scale Thermal Destruction of Per- and Polyfluoroalkyl Substances in a Legacy Aqueous Film Forming Foam. *ACS EST Engg.* **2023,** *3*, (9), 1308-1317. DOI: 10.1021/acsestengg.3c00098
30. National Foam, Inc., Material Safety Data Sheet: Aer-O-Water 3EM 3%, October 1, 2007
31. Shields, E. P.; Wallace, M. A. G., Low temperature destruction of gas-phase per- and polyfluoroalkyl substances using an alumina-based catalyst. *J Air Waste Manag Assoc* **2023,** *73*, (7), 525-532. DOI: 10.1080/10962247.2023.2210103
32. Wu, B.; Hao, S.; Choi, Y.; Higgins, C. P.; Deeb, R.; Strathmann, T. J., Rapid Destruction and Defluorination of Perfluorooctanesulfonate by Alkaline Hydrothermal Reaction. *Environ. Sci. Technol. Lett.* **2019,** *6*, (10), 630-636. DOI: 10.1021/acs.estlett.9b00506
33. Wang, Y.; Pierce, R. D.; Shi, H.; Li, C.; Huang, Q., Electrochemical degradation of perfluoroalkyl acids by titanium suboxide anodes. *Environ. Sci.: Water Res. Technol.* **2020,** *6*, (1), 144-152. DOI: 10.1039/c9ew00759h
34. Sasi, P. C.; Alinezhad, A.; Yao, B.; Kubatova, A.; Golovko, S. A.; Golovko, M. Y.; Xiao, F., Effect of granular activated carbon and other porous materials on thermal decomposition of per- and polyfluoroalkyl substances: Mechanisms and implications for water purification. *Water Res* **2021,** *200*, 117271. DOI: 10.1016/j.watres.2021.117271
35. Ellis, D. A.; Martin, J. W.; De Silva, A. O.; Mabury, S. A.; Hurley, M. D.; Sulbaek Andersen, M. P.; Wallington, T. J., Degradation of fluorotelomer alcohols: a likely atmospheric source of perfluorinated carboxylic acids. *Environ Sci Technol* **2004,** *38*, (12), 3316-21. DOI: 10.1021/es049860w
36. Singh, R. K.; Fernando, S.; Baygi, S. F.; Multari, N.; Thagard, S. M.; Holsen, T. M., Breakdown Products from Perfluorinated Alkyl Substances (PFAS) Degradation in a Plasma-Based Water Treatment Process. *Environ Sci Technol* **2019,** *53*, (5), 2731-2738. DOI: 10.1021/acs.est.8b07031
37. Feng, M.; Qu, R.; Wei, Z.; Wang, L.; Sun, P.; Wang, Z., Characterization of the thermolysis products of Nafion membrane: A potential source of perfluorinated compounds in the environment. *Sci Rep* **2015,** *5*, 9859. DOI: 10.1038/srep09859
38. Altarawneh, M., A chemical kinetic model for the decomposition of perfluorinated sulfonic acids. *Chemosphere* **2021,** *263*, 128256. DOI: 10.1016/j.chemosphere.2020.128256
39. Altarawneh, M.; Almatarneh, M. H.; Dlugogorski, B. Z., Thermal decomposition of perfluorinated carboxylic acids: Kinetic model and theoretical requirements for PFAS incineration. *Chemosphere* **2022,** *286*, (Pt 2), 131685. DOI: 10.1016/j.chemosphere.2021.131685
40. Blotevogel, J.; Giraud, R. J.; Rappé, A. K., Incinerability of PFOA and HFPO-DA: Mechanisms, kinetics, and thermal stability ranking. *Chem. Eng. J.* **2023,** *457*, 141235. DOI: 10.1016/j.cej.2022.141235
41. Khan, M. Y.; So, S.; da Silva, G., Decomposition kinetics of perfluorinated sulfonic acids. *Chemosphere* **2020,** *238*, 124615. DOI: 10.1016/j.chemosphere.2019.124615

42. LaZerte, J. D.; Hals, L. J.; Reid, T. S.; Smith, G. H., Pyrolyses of the Salts of the Perfluoro Carboxylic Acids1. *J. Am. Chem. Soc.* **1953,** *75*, (18), 4525-4528. DOI: 10.1021/ja01114a040
43. Alinezhad, A.; Challa Sasi, P.; Zhang, P.; Yao, B.; Kubátová, A.; Golovko, S. A.; Golovko, M. Y.; Xiao, F., An Investigation of Thermal Air Degradation and Pyrolysis of Per- and Polyfluoroalkyl Substances and Aqueous Film-Forming Foams in Soil. *ACS EST Engg.* **2022**. DOI: 10.1021/acsestengg.1c00335
44. Xiao, F.; Sasi, P. C.; Alinezhad, A.; Golovko, S. A.; Golovko, M. Y.; Spoto, A., Thermal Decomposition of Anionic, Zwitterionic, and Cationic Polyfluoroalkyl Substances in Aqueous Film-Forming Foams. *Environ Sci Technol* **2021,** *55*, (14), 9885-9894. DOI: 10.1021/acs.est.1c02125
45. Yao, B.; Sun, R.; Alinezhad, A.; Kubátová, A.; Simcik, M. F.; Guan, X.; Xiao, F., The first quantitative investigation of compounds generated from PFAS, PFAS-containing aqueous film-forming foams and commercial fluorosurfactants in pyrolytic processes. *J. Hazard. Mater.* **2022,** *436*, 129313. DOI: 10.1016/j.jhazmat.2022.129313
46. Weber, N. H.; Delva, C. S.; Stockenhuber, S. P.; Grimison, C. C.; Lucas, J. A.; Mackie, J. C.; Stockenhuber, M.; Kennedy, E. M., Thermal Decomposition of Perfluorooctanesulfonic Acid (PFOS) in the Presence of Water Vapor. *Ind. Eng. Chem. Res.* **2022,** *61*, (41), 15146-15155. DOI: 10.1021/acs.iecr.2c02463
47. Duchesne, A. L.; Brown, J. K.; Patch, D. J.; Major, D.; Weber, K. P.; Gerhard, J. I., Remediation of PFAS-Contaminated Soil and Granular Activated Carbon by Smoldering Combustion. *Environ Sci Technol* **2020,** *54*, (19), 12631-12640. DOI: 10.1021/acs.est.0c03058
48. Weber, N. H.; Delva, C. S.; Stockenhuber, S. P.; Grimison, C. C.; Lucas, J. A.; Mackie, J. C.; Stockenhuber, M.; Kennedy, E. M., Thermal Mineralization of Perfluorooctanesulfonic Acid (PFOS) to HF, CO2, and SO2. *Ind. Eng. Chem. Res.* **2023**, Ahead of Print. DOI: 10.1021/acs.iecr.2c03197
49. Lyon, R. Method for the Reduction of the Concentration of NO in Combustion Effluents Using Ammonia. US 3,900,554, Aug. 19, 1975.
50. Arand, J. K.; Muzio, L. J.; Sotter, J. G. Urea Reduction of NOx in Combustion Effluents. US 4,208,386, Jun. 17, 1980.
51. Lyon, R. K., Thermal DeNOx Controlling nitrogen oxides emissions by a noncatalytic process. *Environ. Sci. Technol.* **1987,** *21*, (3), 231-236. DOI: 10.1021/es00157a002
52. Backe, W. J.; Day, T. C.; Field, J. A., Zwitterionic, cationic, and anionic fluorinated chemicals in aqueous film forming foam formulations and groundwater from U.S. military bases by nonaqueous large-volume injection HPLC-MS/MS. *Environ Sci Technol* **2013,** *47*, (10), 5226-34. DOI: 10.1021/es3034999
53. U.S. Environmentlal Protection Agency. Performance standards. 40 CFR 264.343, **2024**.
54. Interim Guidance on the Destruction and Disposal of Perfluoroalkyl and Polyfluoroalkyl Substances and Materials Containing Perfluoroalkyl and Polyfluoroalkyl Substances — Version 2 (2024). https://www.epa.gov/system/files/documents/2024-04/2024-interim-guidance-on-pfas-destruction-and-disposal.pdf, Accessed 2024. U.S. EPA 2024
55. Che, S. C.; Iaquaniello, G.; Olivieri, L., Selection of refractory for thermal oxidizers on gas streams containing fluorine. *Environ. Prog.* **2002,** *21*, (2), 116-120. DOI: https://doi.org/10.1002/ep.670210214

APPENDIX A SUPPORTING DATA

Table A1 shows that the results from the OTM-50 samples are very reproducible. The two canisters were sampled in series from the same OTM-50 train during the incineration of the fluorotelomer AFFF.

Table A1. OTM-50 replicate canisters from the incineration of the fluorotelomer AFFF

Temperature (°C)	**1160**	**1160**	**760**	**760**
Compounds	$\mu g/m^3$	$\mu g/m^3$	$\mu g/m^3$	$\mu g/m^3$
Tetrafluoromethane	BDL	BDL	BDL	BDL
Hexafluoroethane	BDL	1.20	11.25	11.49
Chlorotrifluoromethane	BDL	BDL	1.94	2.14
Trifluoromethane	BDL	BDL	1187	1105
Octafluoropropane	BDL	BDL	40.65	41.20
Difluoromethane	BDL	BDL	2.44	2.53
1,1,1,2,2-Pentafluoroethane	BDL	BDL	417.0	414.3
1,1,2,2,3,3,4,4-Octafluorocyclobutane	BDL	BDL	BDL	0.51
Fluoromethane	BDL	BDL	BDL	BDL
Tetrafluoroethylene	BDL	BDL	22.74	23.45
Hexafluoropropene	BDL	BDL	10.57	11.34
1,1,1-trifluoroethane	BDL	BDL	5.30	5.28
Hexafluoropropene Oxide	BDL	BDL	BDL	BDL
Chlorodifluoromethane	0.21	BDL	BDL	BDL
1,1,1,2-Tetrafluoroethane	BDL	BDL	BDL	1.83
Decafluorobutane	BDL	BDL	42.06	43.61
1,1,1,2,2,3,3-Heptafluoropropane	BDL	BDL	59.87	60.13
Octafluorocyclopentene	BDL	BDL	BDL	BDL
Trichlorofluoromethane	0.34	BDL	BDL	0.70
Dodecafluoro-n-pentane	BDL	BDL	6.05	5.91
1,1,1,2,2,3,3,4,4-Nonafluorobutane	BDL	BDL	57.91	60.34
Tetradecafluorohexane	BDL	BDL	BDL	0.87
1,1,1,2,2,3,3,4,4,5,5-Undecafluoropentane	BDL	BDL	32.36	32.18
Heptafluoropropyl 1,2,2,2-tetrafluoroethyl ether	BDL	BDL	BDL	BDL
Hexadecafluoroheptane	BDL	BDL	BDL	BDL
1,1,1,2,2,3,3,4,4,5,5,6,6-Tridecafluorohexane	BDL	BDL	32.43	22.96
Octadecafluorooctane	BDL	BDL	BDL	BDL
1,1,1,2,2,3,3,4,4,5,5,6,6,7,7-Pentadecafluoroheptane	BDL	BDL	BDL	3.79
1,1,1,2,2,3,3,4,4,5,5,6,6,7,7,8,8-Heptadecafluorooctane	BDL	BDL	21.80	20.99
2H-Perfluoro-5-methyl-3,6-dioxanonane	BDL	BDL	BDL	BDL

APPENDIX B LIST OF SCIENTIFIC/TECHNICAL PUBLICATIONS

Krug, J. D.; Lemieux, P. M.; Lee, C. W.; Ryan, J. V.; Kariher, P. H.; Shields, E. P.; Wickersham, L. C.; Denison, M. K.; Davis, K. A.; Swensen, D. A.; Burnette, R. P.; Wendt, J. O. L.; Linak, W. P., Combustion of C1 and C2 PFAS: Kinetic modeling and experiments. *J Air Waste Manag Assoc* **2022**, 72, (3), 256-270. DOI: 10.1080/10962247.2021.202131

Shields, E. P.; Krug, J. D.; Roberson, W. R.; Jackson, S. R.; Smeltz, M. G.; Allen, M. R.; Burnette, R. P.; Nash, J. T.; Virtaranta, L.; Preston, W.; Liberatore, H. K.; Wallace, M. A. G.; Ryan, J. V.; Kariher, P. H.; Lemieux, P. M.; Linak, W. P., Pilot-Scale Thermal Destruction of Per- and Polyfluoroalkyl Substances in a Legacy Aqueous Film Forming Foam. *ACS EST Engg*. **2023**, 3, (9), 1308-1317. DOI: 10.1021/acsestengg.3c00098

Supported the writing of Appendix A in:
US EPA. Interim Guidance on the Destruction and Disposal of Perfluoroalkyl and Polyfluoroalkyl Substances and Materials Containing Perfluoroalkyl and Polyfluoroalkyl Substances — Version 2 (2024). https://www.epa.gov/system/files/documents/2024-04/2024-interim-guidance-on-pfas-destruction-and-disposal.pdf, Accessed 2024. U.S. EPA 2024

Future publication:

Pilot Scale Thermal Destruction of a Per- and Polyfluoroalkyl Substances in a Fluorotelomer Based Aqueous Film Forming Foam, *to be submitted.*

APPENDIX C OTHER SUPPORTING MATERIALS

C.1 FTIR Standard Operating Procedures for UDRI Bench Scale Experiments

System setup

To better understand the SOP and QA/QC parameters described in this document, the system used for the perfluorocarbon (PFC) thermal treatment study is shown in below Figure 1. The calibrated mass flow controllers (MFCs) are used to control both the carrier gases and FCs. The MFCs are calibrated by an ISO 17025-accredited calibration service company prior to the testing. The carrier gases (air and N2) can flow through a reactor or its bypass line. The carrier gases can also flow through a humidifier or its bypass line. The purpose of the humidifier is to supply the hydrogen source to convert liberated F to HF during the thermal treatment study. The effluent gas through the reactor or bypass line is analyzed in situ using an FTIR (MultiGas 2030, MKS).

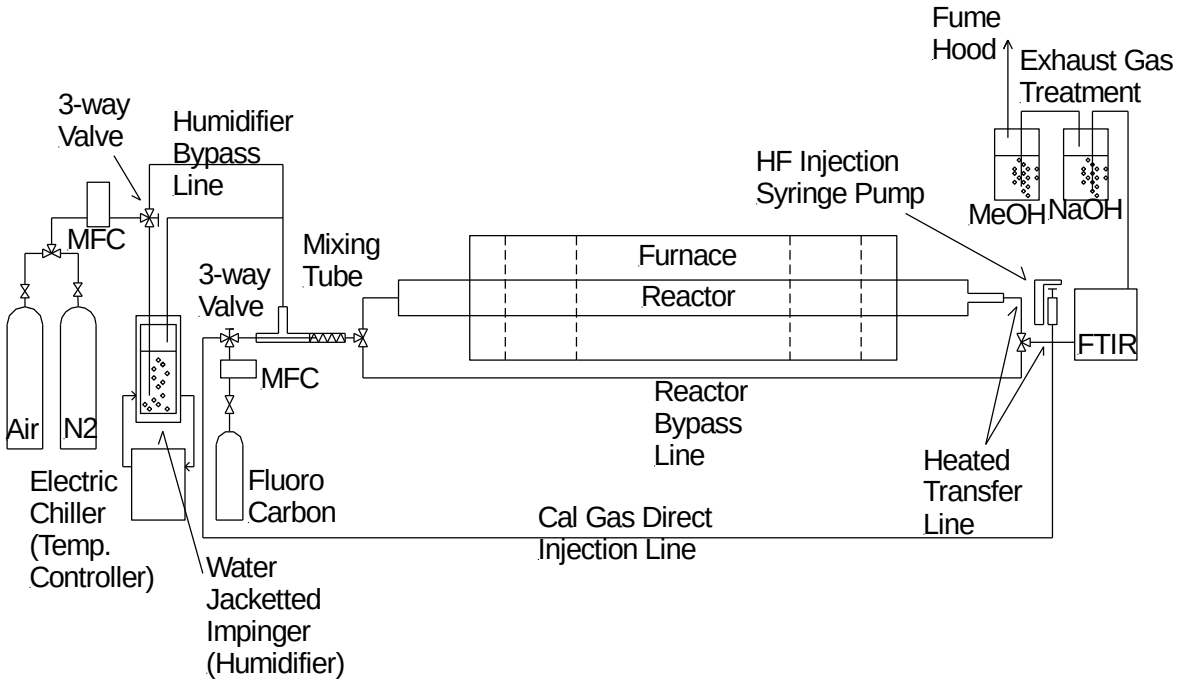

Figure 1. UDRI benchtop experimental system schematic

FTIR Startup

1. Ensure that the Multigas has been switched on for at least 2 hours.
2. Ensure gas cell temperature is within ±2 °C.
3. Flow dry N_2 gas in the gas cell through sample line at 1-2 L/min.
4. Check Multigas optics and modulator N_2 purge (0.2 L/min. for both), even during the experiment.
5. Wait for 20 min. after filling the liquid Nitrogen detector dewar.

6. Go to Multigas software > FT-IR Config Utilities > Instrument Monitor to check the instrument single beam while adding LN_2, to match the reference signal.
7. Wait for 5 min. so that the equilibrium is reached.
8. Go to MultiGas Main > SETUP tap to load the calibration and select the gas recipes, name the gas concentration and spectrum file to store.
9. Go to MultiGas Main > Run.
10. With N_2 still flowing, take a New Background signal, Run> new BKG, (required every 23 hrs), and confirm the minimum signal-to-noise ratio (SNR) shown in Table below:

Table 1. Minimum signal-to-noise ratios for background spectrum

Frequency range for SNR test (cm-1)	Recommended minimum SNR
1000-1100	480
2100-2200	720
2900-3000	480

11. The software automatically checks the SNR and other parameters such as Temperature, Pressure, Laser frequencies, etc. to match the settings, if all the settings match, the final status will be green in the HCU screen under the Health tab, the instrument is fully set up and ready for data acquisition.

Data Acquisition

12. Perform PFAS thermal destruction experiments.
13. Monitor major signals such as parent compounds (if they are in the FTIR calibration database), HF, humidity, and CO2 to reach equilibrium (Table 2 shows the list of chemicals monitored).
14. Acquire the data for 5-10 minutes after reaching the equilibrium.
15. Evaluate data quality using MKS's Analysis Validation Utility software to

a. Determine estimated confidence limits, detection limits, maximum bias, as well as parameters determined using the ASTM Test Method D6348 and EPA Test Method 320
b. Check the measured concentration is above the detection limit
c. Check the measured concentration is within the calibration range
d. Calculate a Standard Deviation (SD)).

16. After experiments, steam clean the system (reactor and FTIR) to remove the remaining HF (below 5 ppm) and PFAS out of the system.

Table 2. Compounds monitored by FTIR

Gas	Upper Limit	Unit
C2F6	999	ppm
CF4	10280	ppm
COF2	5000	ppm
CF2H2	110	ppm
HF	2000	ppm
SiF4	200	ppm
C3F8	1242	ppm
CO2	20	%
H2O	54	%

CO	199199	ppm
C4F10	135	ppm
C5F12	135	ppm
CF3H	999	ppm
SOF2	11030	ppm
SF6	6823	ppm
C3F6	1010	ppm
C5F8	198	ppm

Shutoff/ Idle Procedure

1. Purge the FTIR via the sampling line with dry N_2 at the end of the operation to remove any water and HF residual.
2. N_2 purging can continue overnight until the next experiment or can be stopped after the overnight purge if no FTIR operation is planned.
3. If there is no plan to operate the FTIR for a few days or longer, the instrument can be shutoff by exiting the software and turning the power switch off.

Perfluorocarbon Calibration Procedure

We perform four-point calibration at 25, 50, 75, and 125 ppm for C1 – C5 fluorocarbons to examine and correct for any inaccuracy of the FTIR library for those compounds.

1. Follow General FTIR SOP 1 to 11.
2. Flow the carrier gas to the bypass line using the certified Mass Flow Controller (MFC) with the effective calibration certificate.
3. Flow the C1 – C5 fluorocarbons individually to the bypass line using the MFC with the effective calibration certificate.
4. Introduce the gas mixture to FTIR.
5. Monitor C1 – C5 fluorocarbon concentrations to reach equilibrium.
6. Acquire the data for 5-10 minutes after reaching the equilibrium.
7. Evaluate data quality using MKS's Analysis Validation Utility software (General FTIR SOP Step 15).
8. Develop the calibration curve by fitting them with either linear or quadratic fit.

HF Calibration Procedure

We perform four-point calibration at 500, 1000, 1500, and 2000 ppm for HF to examine and correct for any inaccuracy of the HF FTIR library. To avoid HF reaction with the fused silica quartz tube and the transfer line, the HF solution will be directly injected into the heated transfer line in front of the FTIR.

1. Follow General FTIR SOP 1 to 11.
2. Prepare HF solution in Deionized (DI) Water.

3. Measure fluoride (F^-) concentration using the calibrated F^- analyzer with the effective calibration certificate to confirm the measured F^- concentration is consistent with the expected F^- concentration.
4. Heat the furnace temperature at 200 °C and flow the N_2 gas to the reactor using the certified MFC with the effective calibration certificate.
5. Introduce and vaporize the HF solution in the FTIR transfer line using the certified and calibrated syringe pump.
6. Introduce the gas mixture to FTIR.
7. Monitor HF concentrations to reach equilibrium.
8. Acquire the data for 5-10 minutes after reaching the equilibrium.
9. Evaluate data quality using MKS's Analysis Validation Utility software (General FTIR SOP Step 15).
10. Develop the calibration curve by fitting them with either linear or quadratic fit.

The following QA/QC checks are considered to conduct C1 – C5 PFC thermal treatment study.

Determination of the Bias before and after Each Experiment

1. Use C_2F_6 as a model compound.
2. Set the furnace temperature at the targeted temperature for each experiment.
3. Flow N_2 (Ultra-High Purity, UHP, grade) carrier gas using the calibrated MFC to the bypass line without passing through the humidifier.
4. Flow C_2F_6 with the certificate of Analysis (COA) using the calibrated MFC to the Cal Gas Direct Injection Line.
5. Introduce the gas mixture to FTIR.
6. Wait until the FTIR signal is stabilized. Measure the fluorocarbon concentration with FTIR.
7. The bias (B) is the difference between the calculated concentration and measured concentration using FTIR. If the relative bias is less than or equal to 10 percent, the bias of the candidate test method is acceptable.
8. Calculate the Correction Factor (CF) as follows:

$$CF = \frac{1}{1+\frac{B}{CS}} \qquad \text{---------- (1)}$$

B: Bias

CS: Calculated Value

9. Analytical results of the test method are multiplied by the correction factor, if $0.7 \leq CF \leq 1.3$. If it is determined that the bias is significant and CF > ±30 percent, then the test method is considered to be "not valid."
10. If the Bias is different before and after the experiment, take the larger value as a bias.
    -

Determination of C1 – C5 PFC Thermal Decomposition Efficiency

Besides B and CF calculations, C1 – C5 PFC Thermal Decomposition Efficiencies (TDEs) are calculated as follows so that FTIR's Sample-Independent Factors are canceled out as much as possible:

1. Flow air using the calibrated MFC to the bypass line without passing through a humidifier.
2. Flow individual C1 – C5 fluorocarbons with the certificate of Analysis (COA) using the calibrated MFC to the bypass line.
3. Wait until the FTIR signal is stabilized. Measure the fluorocarbon concentration with FTIR. This is the Base Line (BL) concentration.
4. Flow air using the calibrated MFC to the reactor by passing through a humidifier.
5. Flow individual C1 – C5 FCs with COA using the calibrated MFC to the reactor.
6. Measure the FC concentration with FTIR. This is the Experimental Concentration (EC) value.
7. Calculate the TDE of the C1 – C5 FC as follows:

$$TDE = (1 - \frac{EC}{BL}) \times 100\ (\%) \qquad \text{---------- (2)}$$

EC: Experimental Concentration

BL: Base Line concentration

Data Correction of HF Measurements

It is believed that the best way to avoid sample dependent/independent error to estimate the gas phase HF concentration using FTIR is to perform the HF recovery efficiency (RE) test at each temperature and residence time, and apply RE to the HF value obtained from the experiment. The HF RE test is conducted by injecting the known concentration of HF solution using the syringe pump and nebulizing it at the front end of the reactor as shown in Figure 2. The reason to conduct HF RE for each temperature and residence time is that HF RE is significantly affected by these two factors. HF RE can be calculated as follows:

$$HF\ RE = (\frac{RHF}{CHF}) \qquad \text{---------- (3)}$$

RHF: Recovered HF concentration measured by FTIR

CHF: Calculated HF concentration

The measured HF (MHF) concentrations during the thermal destruction experiment will be corrected as follows to take into account the HF loss during the experiments. The Corrected HF (CorrHF) concentration will be calculated as follows:

$$CorrHF = \frac{MHF}{(HF\ RE)} \qquad \text{---------- (4)}$$

MHF: Measured HF

HF RE: HF Recovery Efficiency

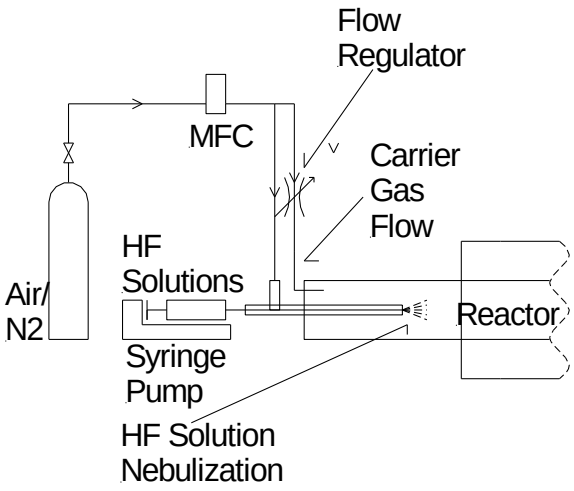

Figure 2. HF injection nebulizer schematic